PNPI - NRC KI

JINR

Modelling polarized atomic beam source (PABS)

V. Larionov, A. Vasilyev, L. Kochenda,
P. Kravtsov, P. Kravchenko, A. Rozhdestvenskij, V. Trofimov, V. Fotyev

Petersburg Nuclear Physics Institute
Gatchina, Russia

K. Ivshin, A. Solovev, V. Fimushkin

Joint Institute for Nuclear Research
Dubna, Russia

PolFusion

Objective and Tasks

Objective:

Creating software for PABS modeling

Tasks:

1. Development of an atomic beam initial condition generator based on the Monte Carlo method.
2. Creation of a numerical model of a multipolar magnetic system
3. Modelling of radio frequency transition blocks

Polarized atomic beam source (PABS)

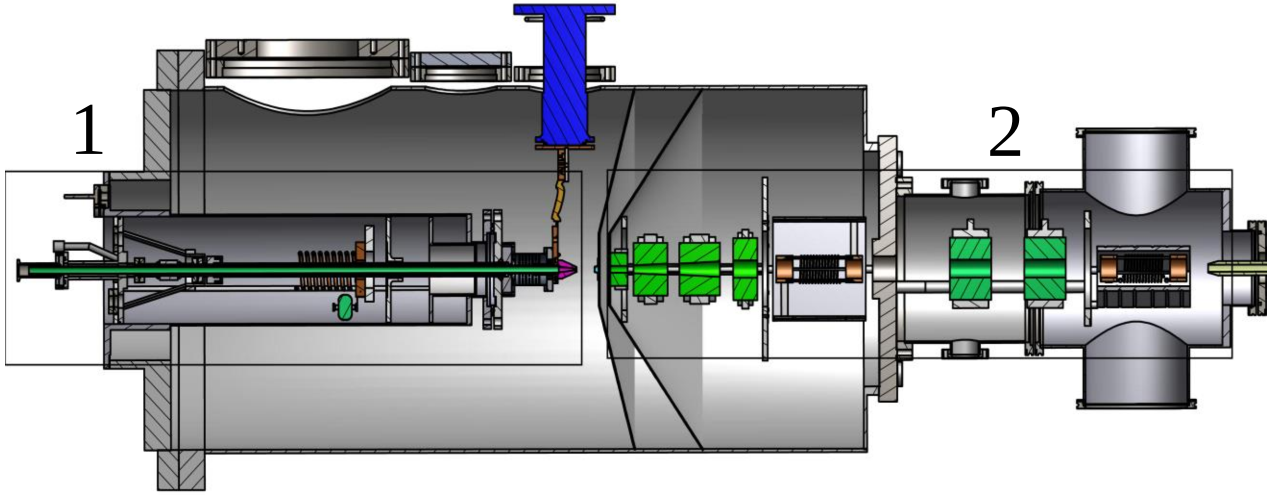

PolFusion polarized atomic beam source

SPI polarized atomic beam source

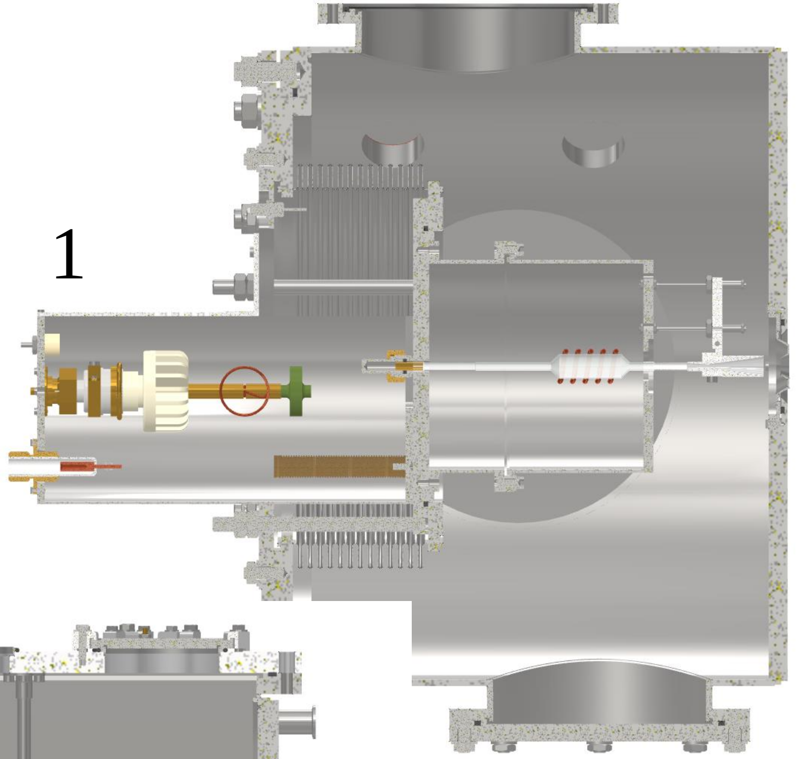

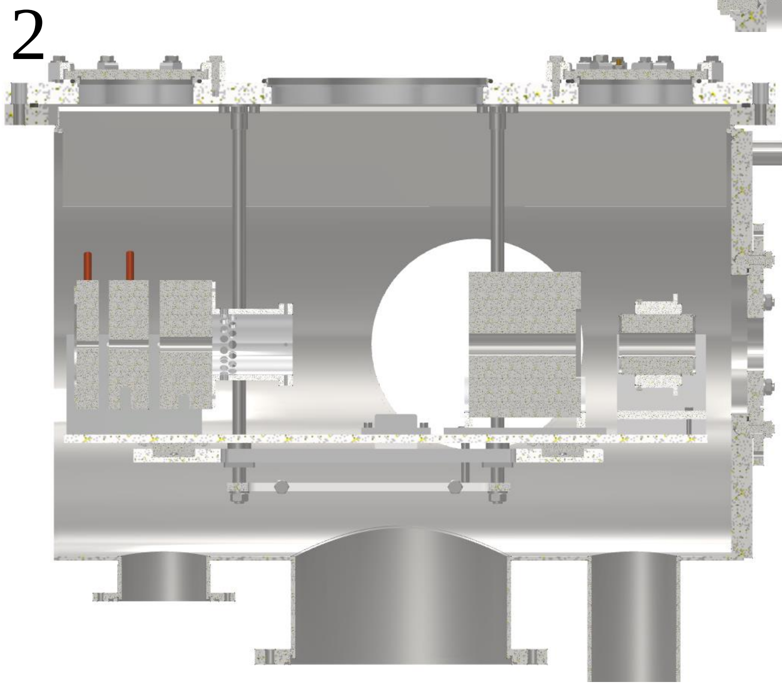

1. Radio frequency dissociator
2. Polarizer

RF - dissociator

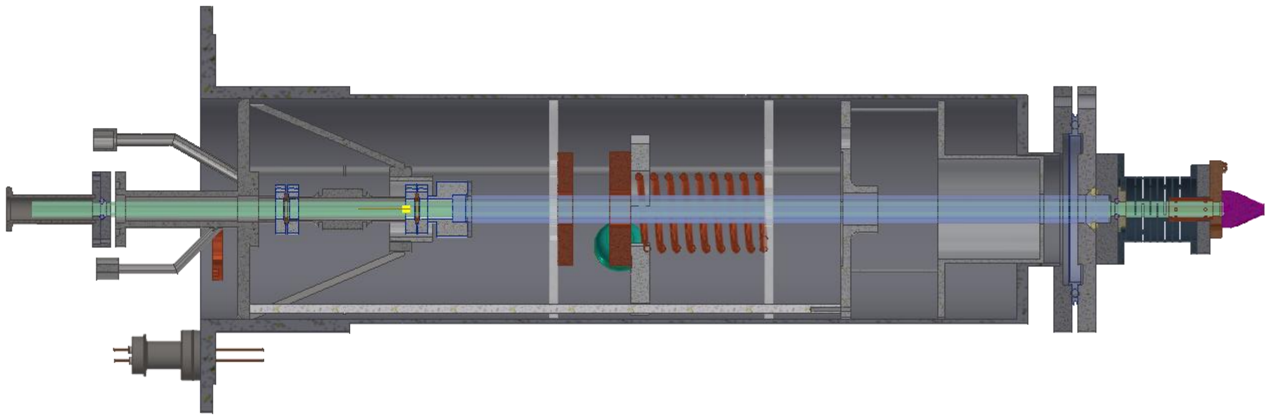

PolFusion dissociator

$f = 13.56MHz$

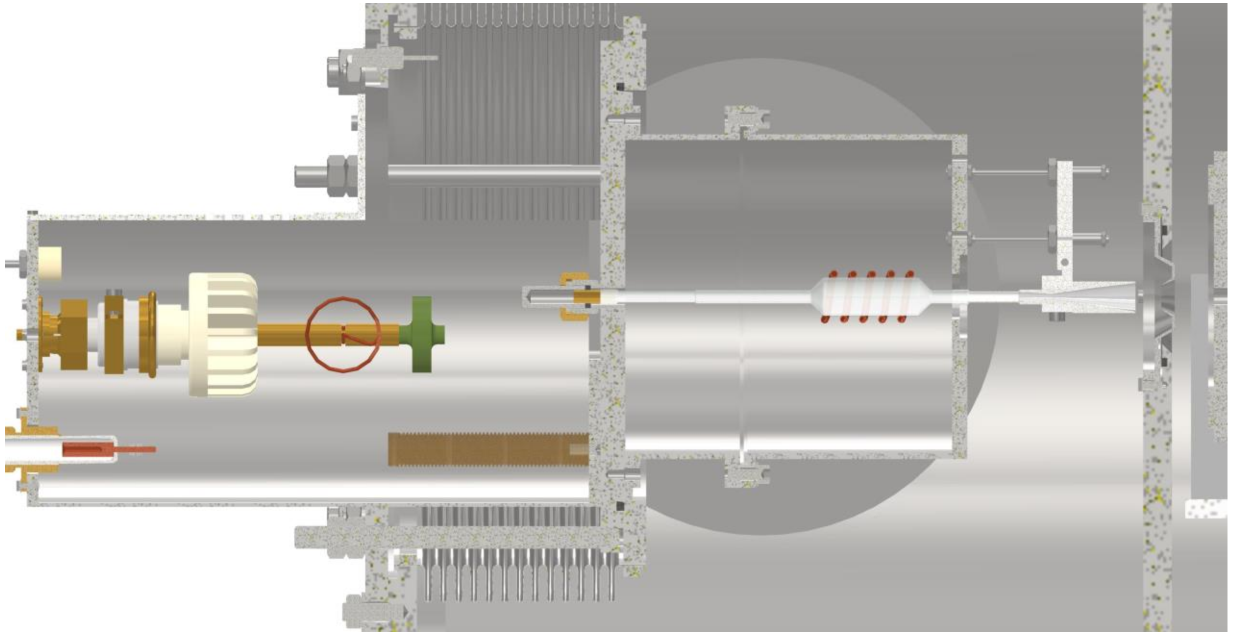

SPI dissociator

$f = 70\ MHz$

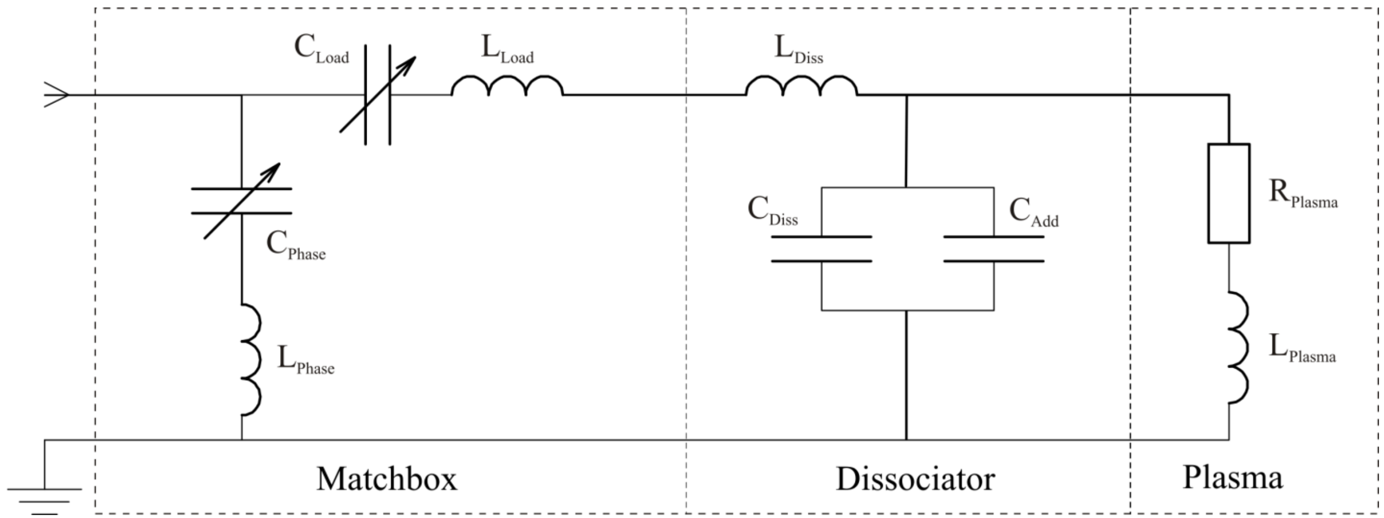

Multipolar magnetic system

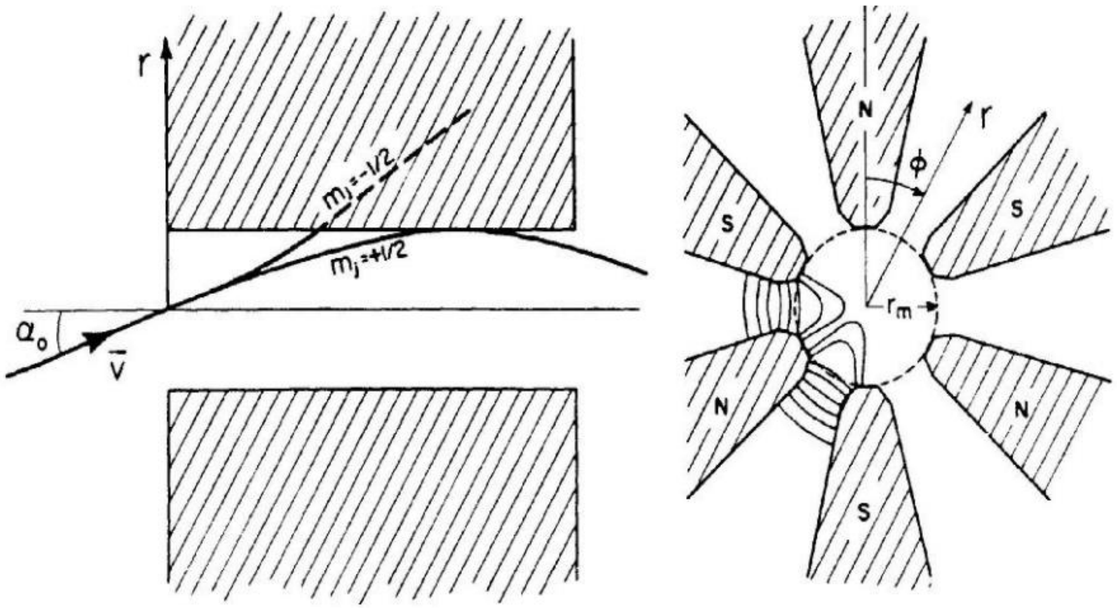

A sextuple magnet used in ABS. An atom flying into a magnet with r = 0 at an angle α_0 is shown on the left; several lines of force are shown on the right

1. $$\frac{d^2\vec{r}^{\,1}}{dt^2} = \frac{1}{m} B_0 \left(\frac{N}{2} - 1\right) \frac{(\mu_e + \mu_d)}{r_0^{\frac{N}{2}-1}}\, r^{\frac{N}{2}-2}$$

2. $$\frac{d^2\vec{r}^{\,2}}{dt^2} = \frac{1}{2m}\left(\mu_d - \frac{-A_d\mu_c + \mu_c^2 B}{\sqrt{9A_d^2 - 2A_d\mu_c B + {\mu_c}^2 B^2}}\right) B_0 \left(\frac{N}{2} - 1\right) \frac{r^{\frac{N}{2}-2}}{r_0^{\frac{N}{2}-1}}$$

3. $$\frac{d^2\vec{r}^{\,3}}{dt^2} = \frac{1}{2m}\left(-\mu_d - \frac{A_d\mu_c + \mu_c^2 B}{\sqrt{9A_d^2 + 2A_d\mu_c B + {\mu_c}^2 B^2}}\right) B_0 \left(\frac{N}{2} - 1\right) \frac{r^{\frac{N}{2}-2}}{r_0^{\frac{N}{2}-1}}$$

4. $$\frac{d^2\vec{r}^{\,4}}{dt^2} = -\frac{1}{m} B_0 \left(\frac{N}{2} - 1\right) \frac{(\mu_e + \mu_d)}{r_0^{\frac{N}{2}-1}}\, r^{\frac{N}{2}-2}$$

5. $$\frac{d^2\vec{r}^{\,5}}{dt^2} = \frac{1}{2m}\left(-\mu_d + \frac{A_d\mu_c + \mu_c^2 B}{\sqrt{9A_d^2 + 2A_d\mu_c B + {\mu_c}^2 B^2}}\right) B_0 \left(\frac{N}{2} - 1\right) \frac{r^{\frac{N}{2}-2}}{r_0^{\frac{N}{2}-1}}$$

6. $$\frac{d^2\vec{r}^{\,6}}{dt^2} = \frac{1}{2m}\left(\mu_d + \frac{-A_d\mu_c + \mu_c^2 B}{\sqrt{9A_d^2 - 2A_d\mu_c B + {\mu_c}^2 B^2}}\right) B_0 \left(\frac{N}{2} - 1\right) \frac{r^{\frac{N}{2}-2}}{r_0^{\frac{N}{2}-1}}$$

Radio - frequency transition cells

$F_{in} - F_{out} = \Delta F = \pm 1{,}0$ and $\Delta m = \pm 1{,}0$

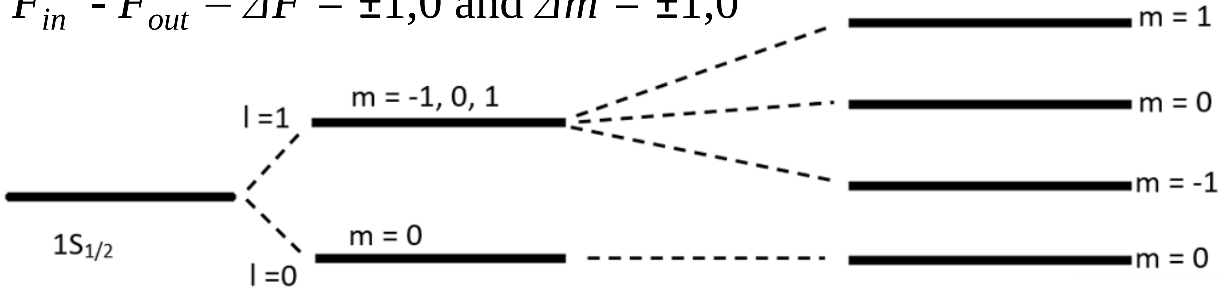

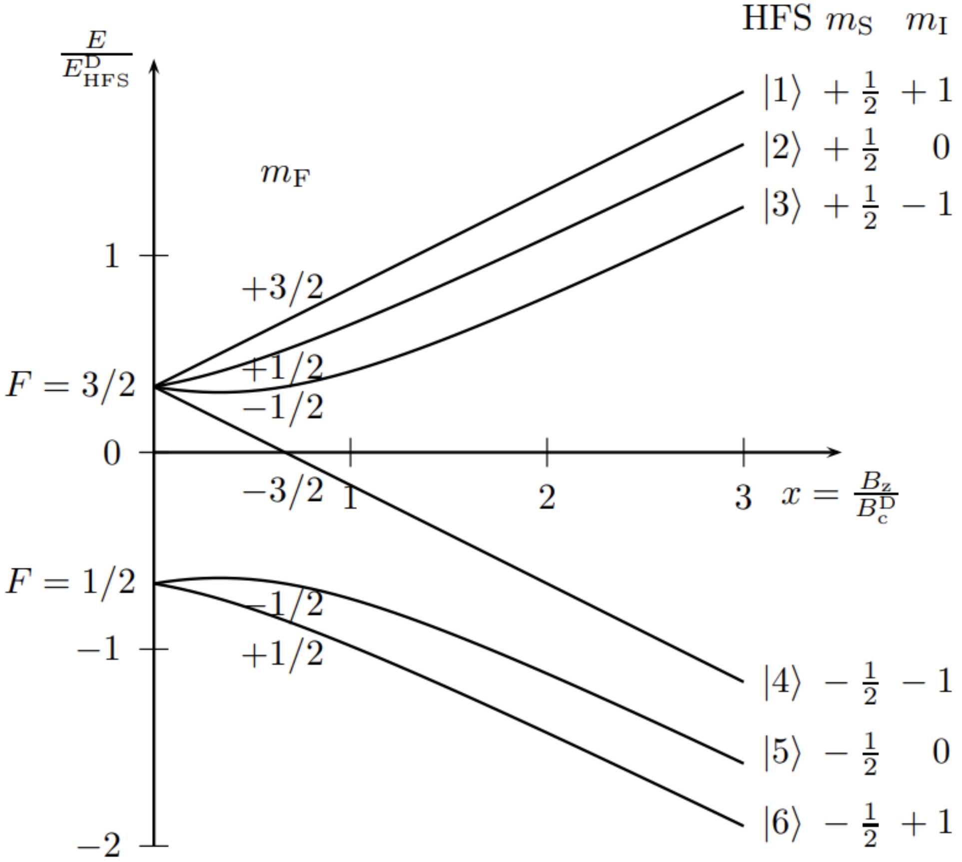

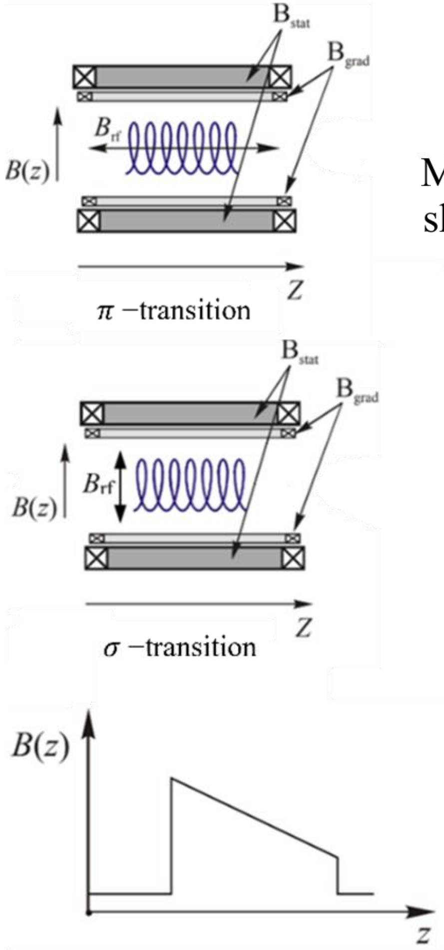

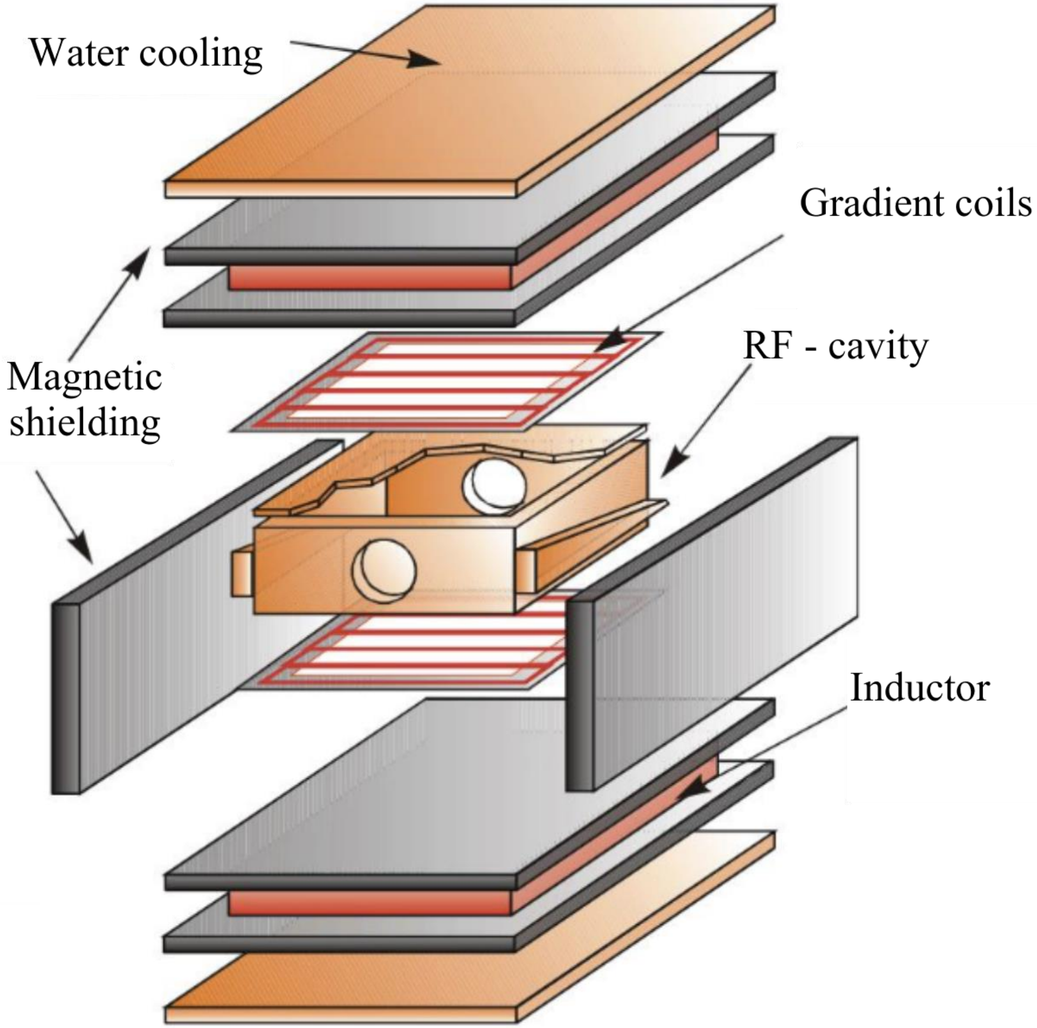

Polarization of the gas target

P_z	P_{zz}	Multipolar magnetic system 1		MFT1	Multipolar magnetic system 2		MFT2	m_i
		Before	After	After	Before	After	After	
0	+1	$\|1\rangle$ $\|2\rangle$ $\|3\rangle$ $\|4\rangle$ $\|5\rangle$ $\|6\rangle$	$\|1\rangle$ $\|2\rangle$ $\|3\rangle$	On $2 \leftrightarrow 4$ $\|1\rangle$ $\|3\rangle$ $\|4\rangle$	$\|1\rangle$ $\|3\rangle$ $\|4\rangle$	$\|1\rangle$ $\|3\rangle$	Off $\|1\rangle$ $\|3\rangle$	+1 -1
-2/3	0	$\|1\rangle$ $\|2\rangle$ $\|3\rangle$ $\|4\rangle$ $\|5\rangle$ $\|6\rangle$	$\|1\rangle$ $\|2\rangle$ $\|3\rangle$	On $\|1\rangle$ $\|2\rangle$ $\|3\rangle$	$\|1\rangle$ $\|2\rangle$ $\|3\rangle$	$\|1\rangle$ $\|2\rangle$ $\|3\rangle$	Off $1 \leftrightarrow 4$ $\|2\rangle$ $\|3\rangle$ $\|4\rangle$	0 -1 -1

Initial data generator

The atomic beam is defined by an event generator that produces a particle with the following parameters:

1. Particle coordinates (z, r)

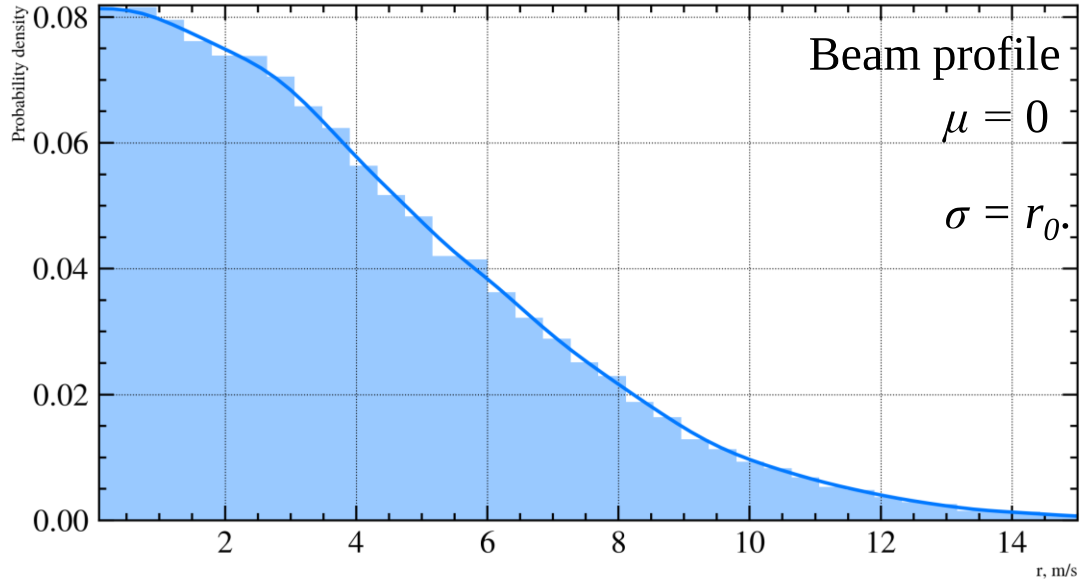

2. The projection of the total atomic spin

The polarization of the particle is defined according to a uniform distribution, so that the initial atomic beam is unpolarized.

3. The velocity of the particle along the OZ axis, v_r, and the velocity along the Or axis, v_z

Velocity distributions

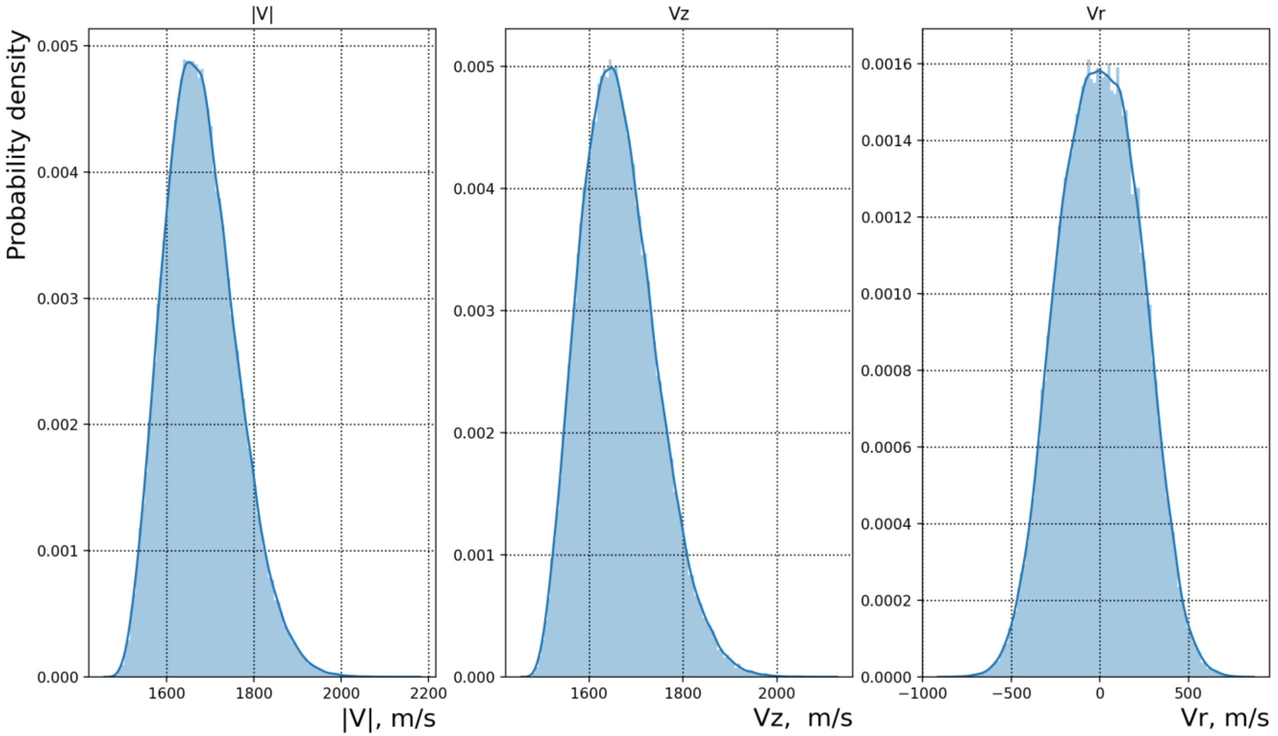

Modelling multipolar magnetic system

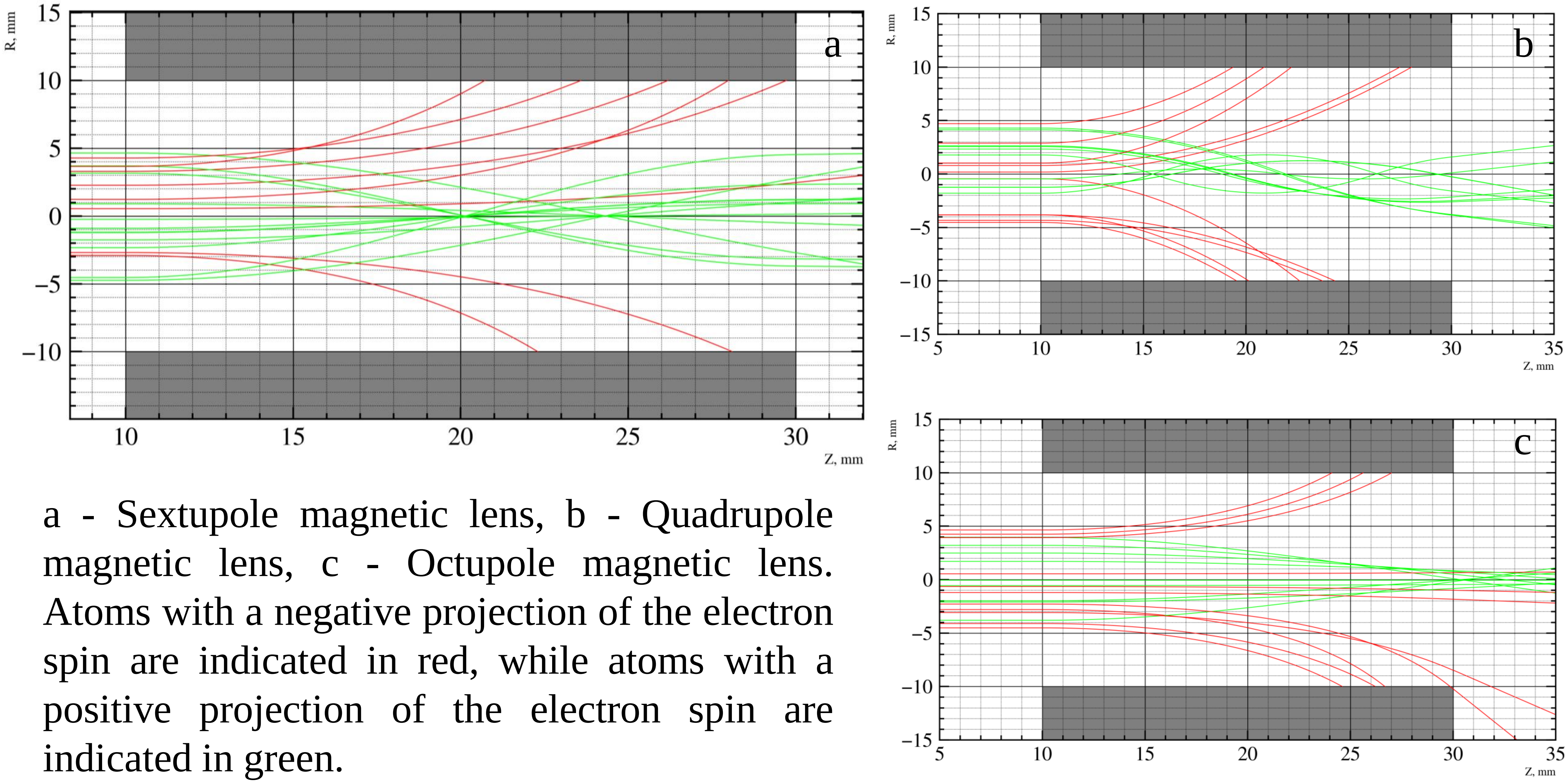

a - Sextupole magnetic lens, b - Quadrupole magnetic lens, c - Octupole magnetic lens. Atoms with a negative projection of the electron spin are indicated in red, while atoms with a positive projection of the electron spin are indicated in green.

Modelling multipolar magnetic system (SPI ABS)

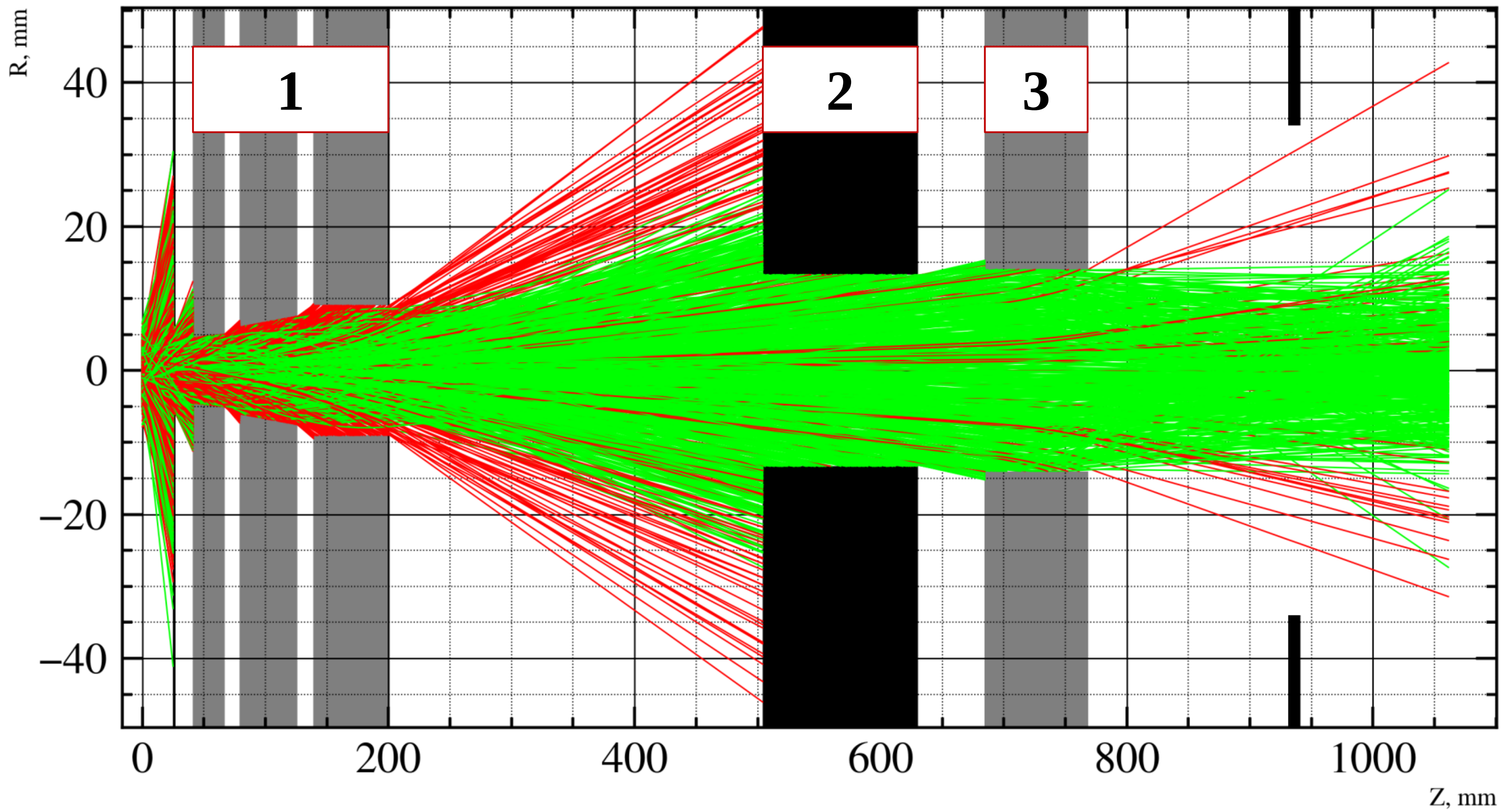

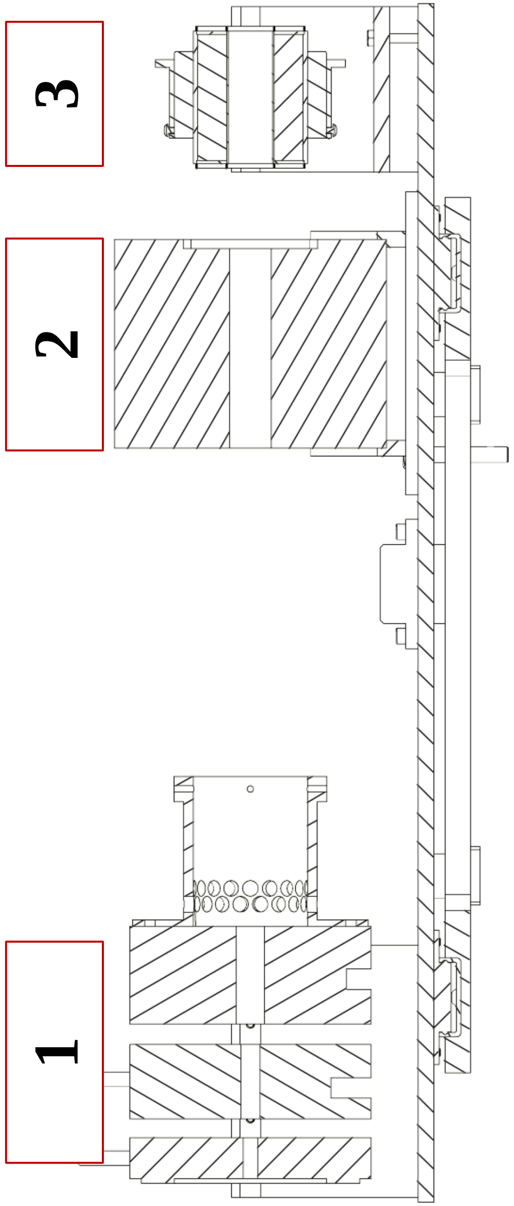

1 - the first three sextupole lenses,
2 - the wall,
3 - the sextupole lens

$$P_{+\frac{1}{2}} = (91.3 \pm 1.4)\%$$

$$\text{Intensity} = \frac{N_{end}}{N_{start}} * 100\%$$

$$\text{Intensity} = (0.36 \pm 0.04)\%$$

Modelling polarizer (PolFusion ABS)

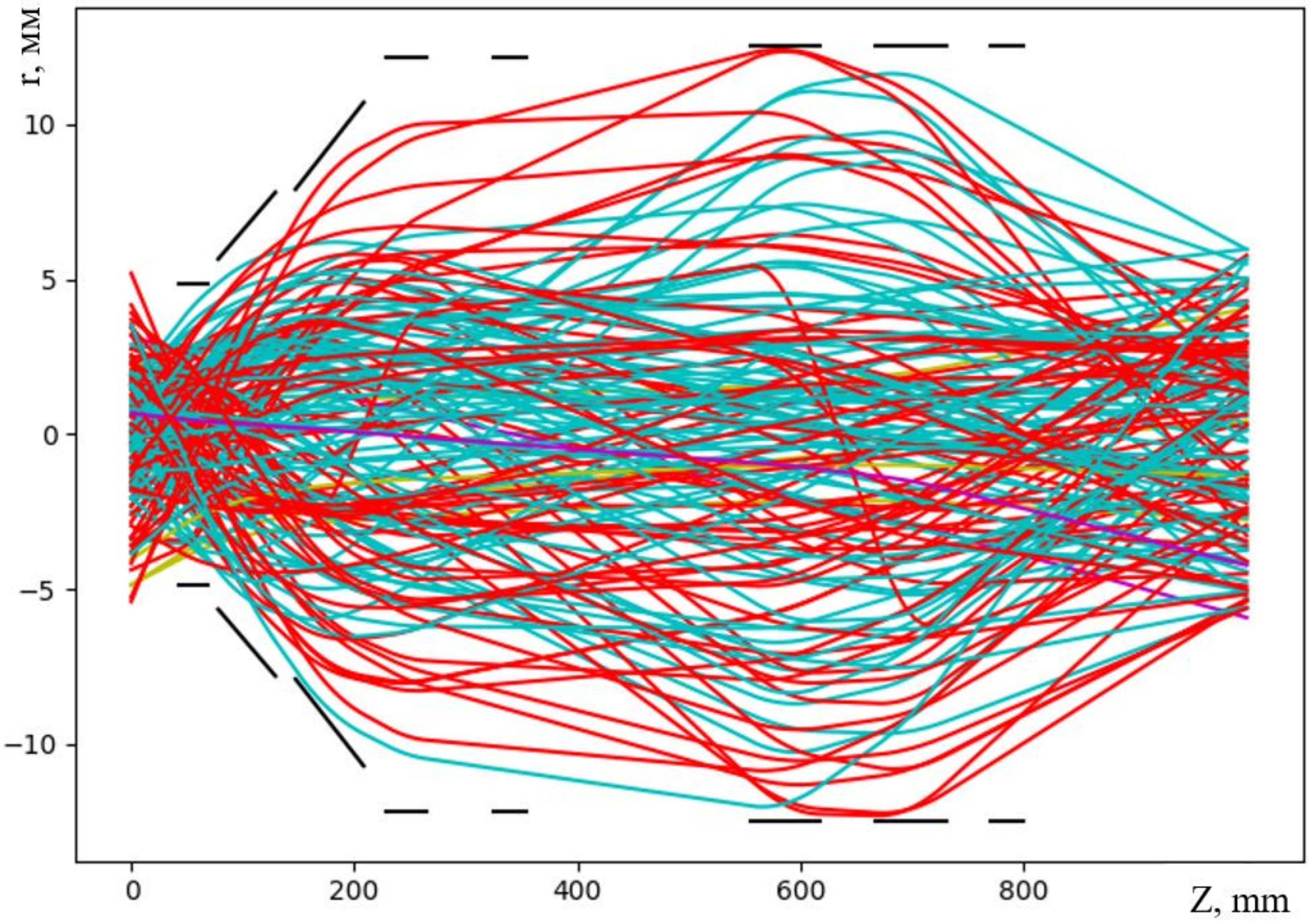

$$P_z(I=1) = \frac{N_{(m_i=+1)} - N_{(m_i=-1)}}{N_{(m_i=+1)} + N_{(m_i=0)} + N_{(m_i=-1)}},$$

$$P_{zz}(I=1) = \frac{1 - 3N_{(m_i=0)}}{N_{(m_i=+1)} + N_{(m_i=0)} + N_{(m_i=-1)}}$$

Color	State
Blue	$\|1\rangle$
Green	$\|2\rangle$
Red	$\|3\rangle$
Cyan	$\|4\rangle$
Purple	$\|5\rangle$
Yellow	$\|6\rangle$

Intensity 0.17%
Vector polarization -0,9
Tensor polarization 0,86

Checking the performance of the polarizer simulation

	$P_{z,\ meas.}$	$P_{zz,\ meas.}$	$P_{z,\ sim.}$	$P_{zz,\ sim.}$
ANKE PABS	+0.88 ± 0.01	+0.88 ±0.03	+0.89 ± 0.03	+0.90 ± 0.03
	-0.91 ±0.01	+0.85 ±0.2	-0.91 ±0.03	+0.89 ± 0.03
	+0.005 ±0.003	+0.90 ±0.02	-0.06 ± 0.08	+0.90 ± 0.04
	+0.005±0.003	-1.71 ± 0.03	-0.08 ± 0.03	-1.58 ± 0.07
HERMES PABS	+0.92 ±0.01	+0.88 ± 0.02	+0.94 ±0.021	+0.89 ± 0.03
	-0.91 ±0.01	+0.94± 0.02	-0.92 ±0.011	+0.95± 0.01
	-0.02± 0.01	+0.99 ± 0.02	-0.05± 0.08	+0.96 ± 0.05
	-0.02±0.01	-1.77 ±0.02	-0.03±0.02	-1.64 ±0.04

Choosing the optimal PABS design (PolFusion)

	$P_{z.\ theor}$	$P_{zz,\ theor}$	$P_{z,\ sim.}$	$P_{zz,\ sim.}$	Intensity, %
Design №1 (6666 66)	0	+1	+0.06 ±0.08	+0.89 ±0.02	0.20 ±0.02
	- 1/3	+1	-0.26 ±0.06	+0.92 ±0.03	0.21 ±0.02
	-1	+1	-0.92 ±0.02	+0.92 ±0.02	0.16 ±0.01
Design №2 (6646 46)	0	+1	-0.46±0.06	+0.86±0.04	0.13±0.01
	- 1/3	+1	-0.63 ±0.05	+0.94 ± 0.03	0.14 ± 0.01
	-1	+1	-0.95±0.02	+0.95±0.04	0.14 ±0.01
Design №3 (8888 88)	0	+1	-0.50 ± 0.05	+0.86 ± 0.05	0.22 ± 0.01
	- 1/3	+1	-0.58 ± 0.07	+0.88±0.03	0.20±0.01
	-1	+1	-0.89±0.03	+0.89±0.04	0.21 ± 0.01

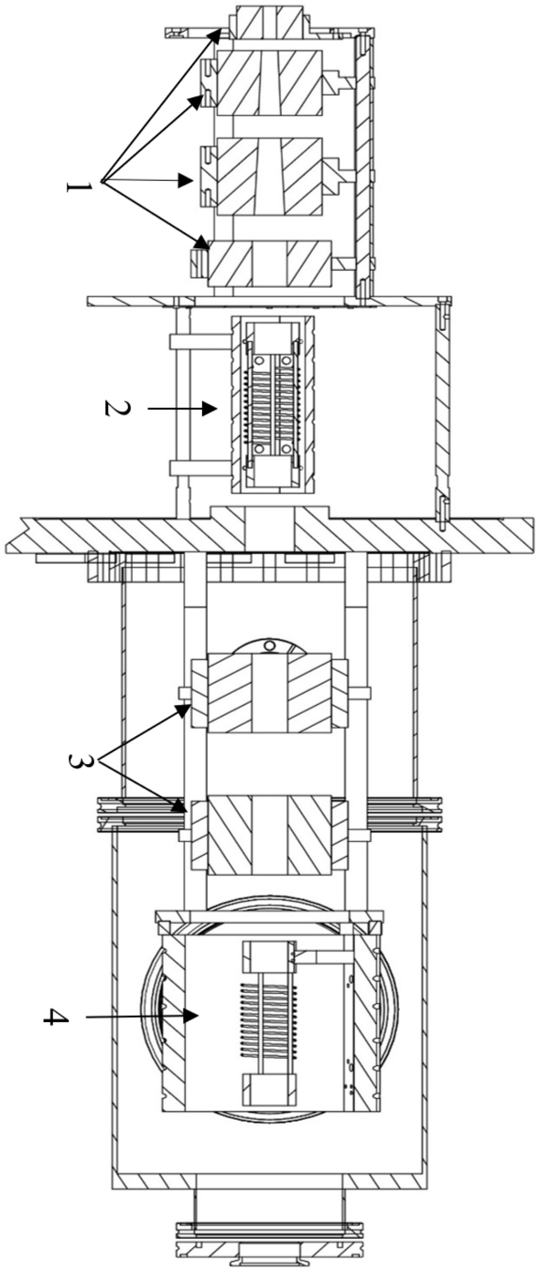

PABS optimization based on nozzle temperature

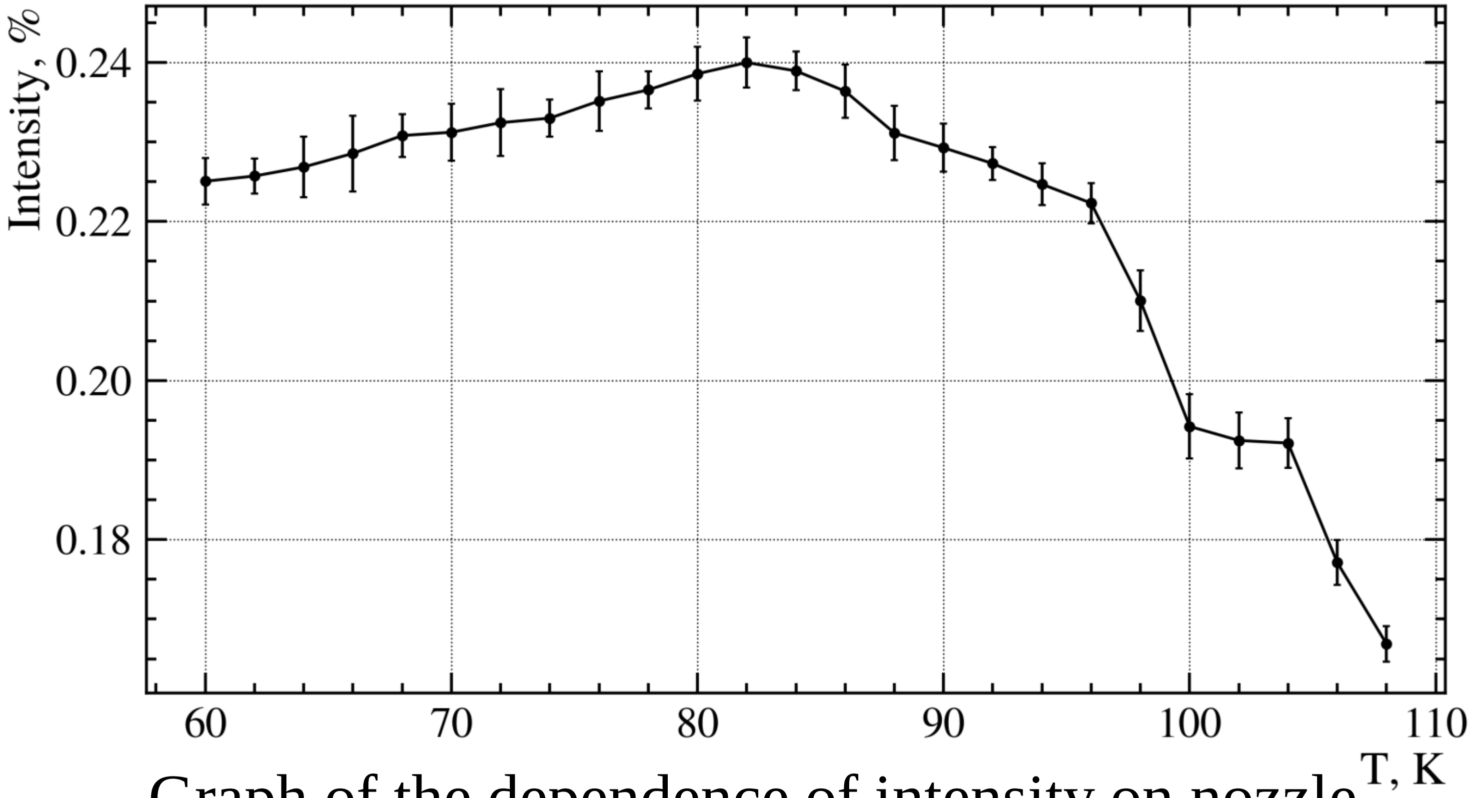

Graph of the dependence of intensity on nozzle temperature (calculated)

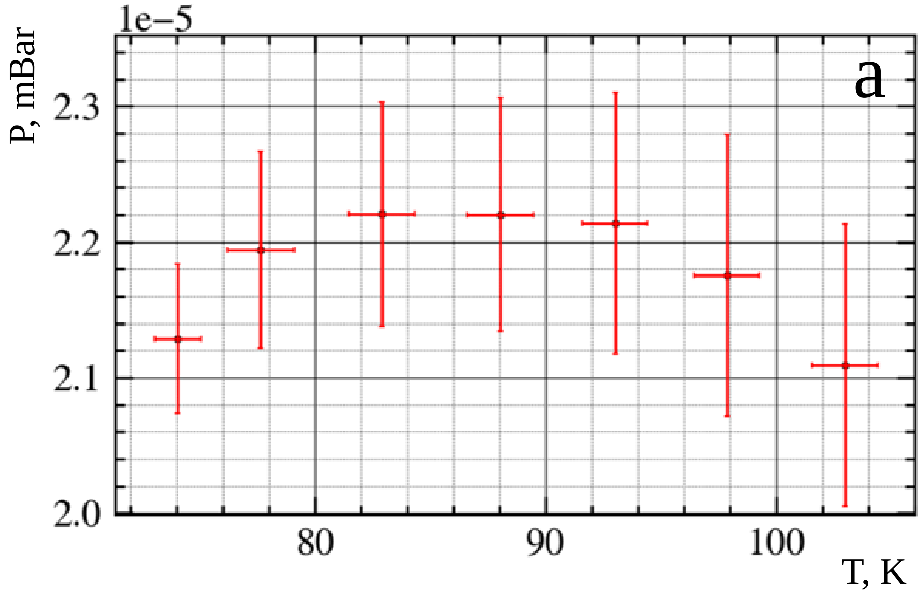

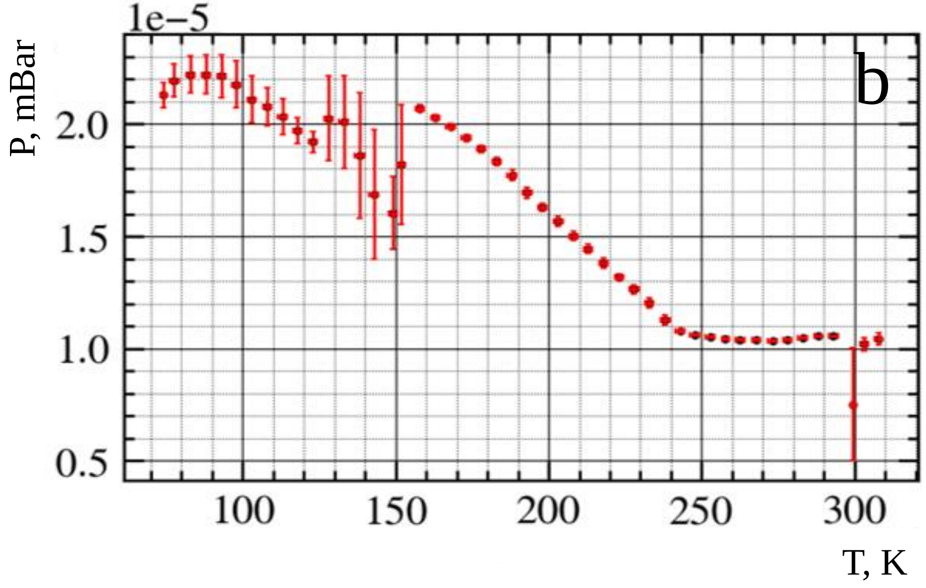

Graph of the dependence of pressure in the compression tube on the nozzle temperature:
a - in the range from 70 to 110 K,
b - in the range from 0 to 310 K.

Conclusion

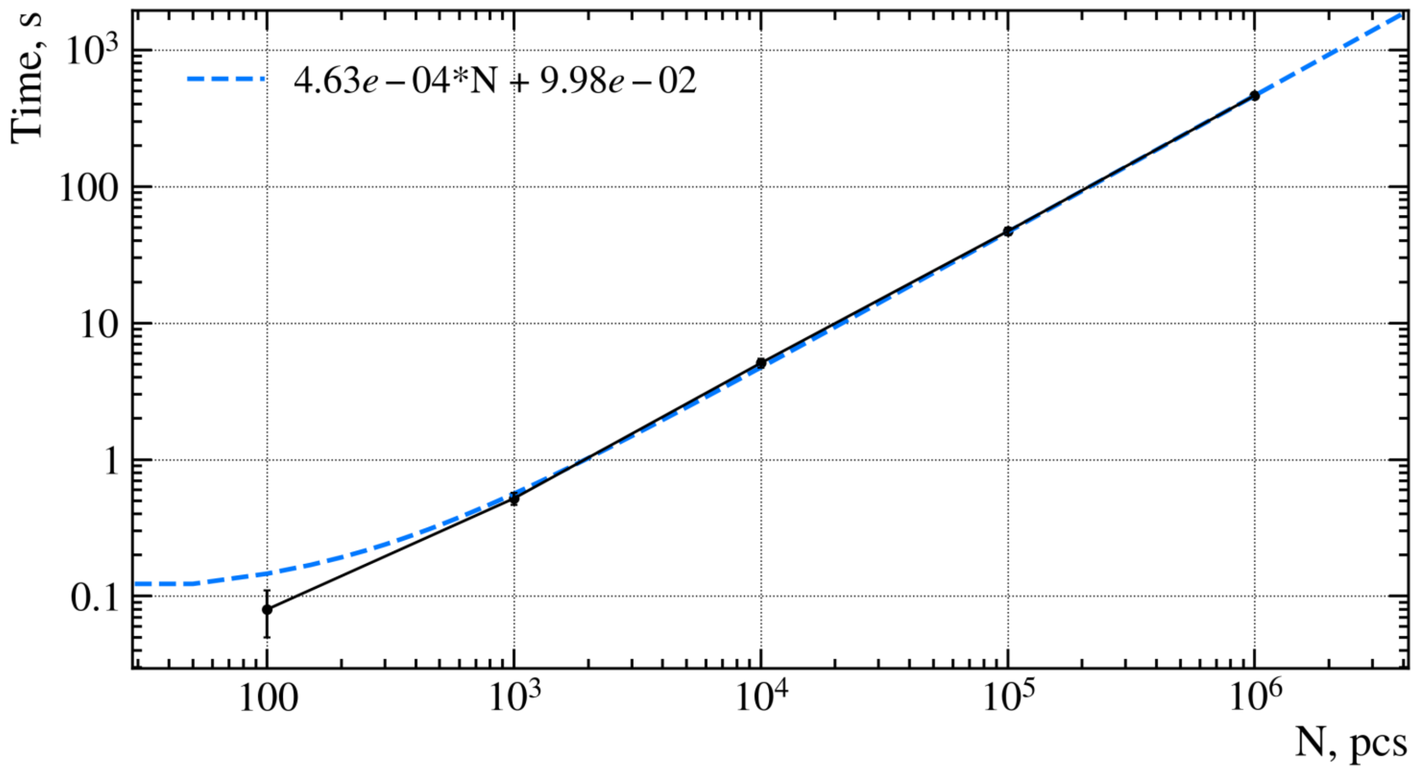

Assumptions

When calculating the passage through the magnet, the following assumptions were made:

1. There are no edge effects at the boundary of the magnet, meaning that the particles travel uniformly and in a straight line towards the magnet.

2. The magnet is infinitely tall.

3. The change in the velocity of the atomic beam along the Z-axis is negligible: $v_z = const$.

1. The intensity calculated during the simulation aligns very closely with the intensity measured in experimental setups.

2. The degree of polarization calculated during the simulation, taking into account the margin of error, falls within the range of experimental data.

3. The runtime complexity of the program is O(n).

Thank you for your attention!

PABS

p_z (vector)	p_{zz} (tensor)
-2/3	0
0	+1
-1/3	+1
-1	+1
±1/2	-1/2

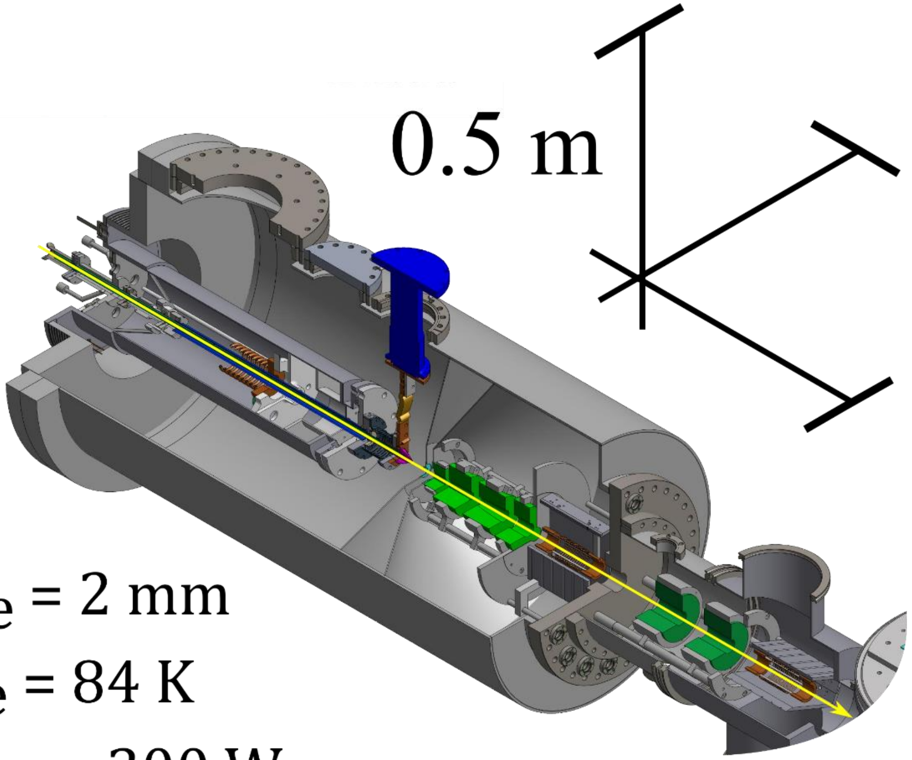

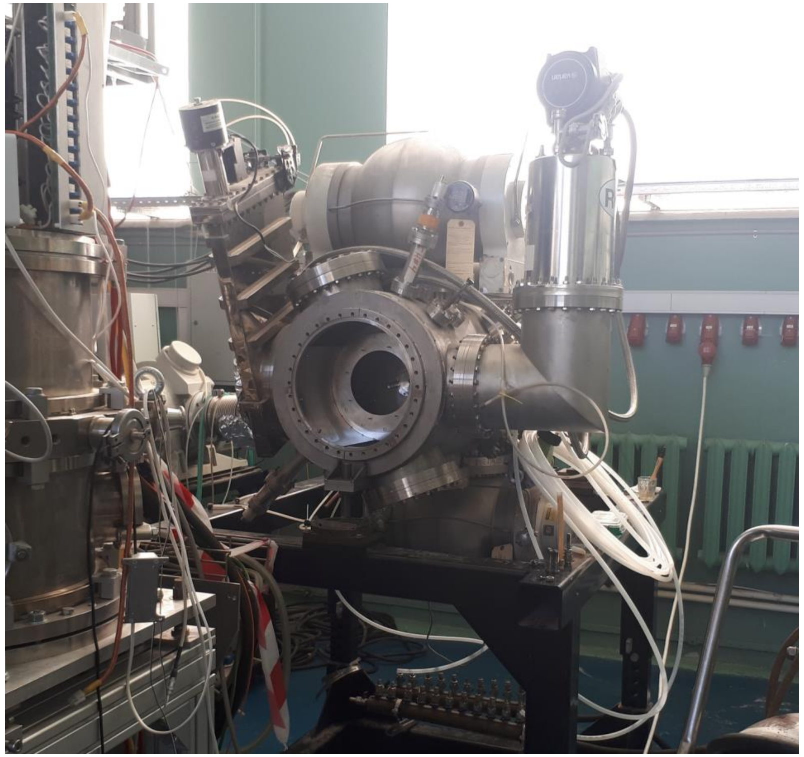

atomic beam d_{nozzle} = 2 mm

$\vec{D}$, 0.01 eV T_{nozzle} = 84 K

$2 \cdot 10^{16}$ atoms/s RF_{power} = 300 W

Polarizing system:

Sextupoles + Quadrupoles + MFT + Sextupoles + MFT

POLIS

p_z (vector)	p_{zz} (tensor)
±2/3	0
0	+1
0	-2
-1/3	±1
+1/3	±1
±1/3	-1/2

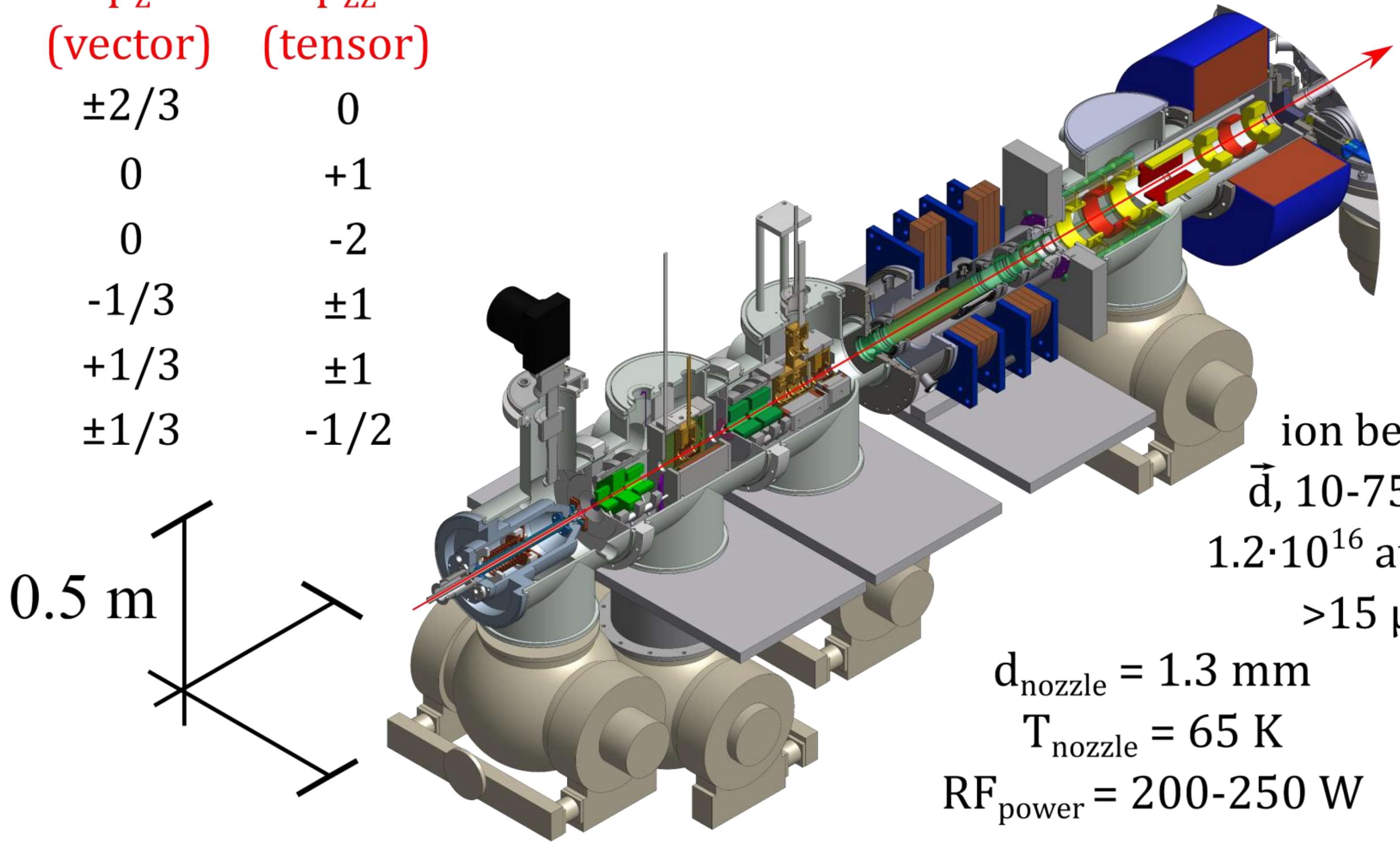

ion beam
$\vec{d}$, 10-75 keV
$1.2 \cdot 10^{16}$ atoms/s
>15 μA

d_{nozzle} = 1.3 mm
T_{nozzle} = 65 K
RF_{power} = 200-250 W

Polarizer:

Sextupoles + WFT + Sextupoles + WFT + SFT1 (460 MHz) +SFT2 (350 MHz)

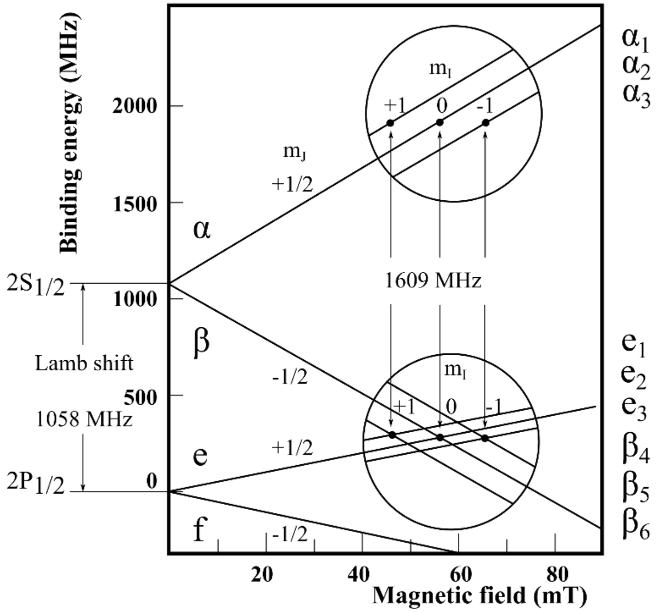

PNPI - NRC KI

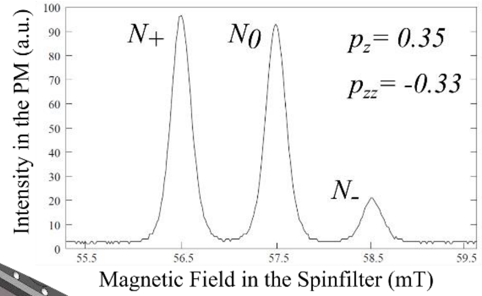

$$p_z = \frac{N_+ - N_-}{N_+ + N_- + N_0},$$

$$p_{zz} = \frac{N_+ + N_- - 2N_0}{N_+ + N_- + N_0}.$$

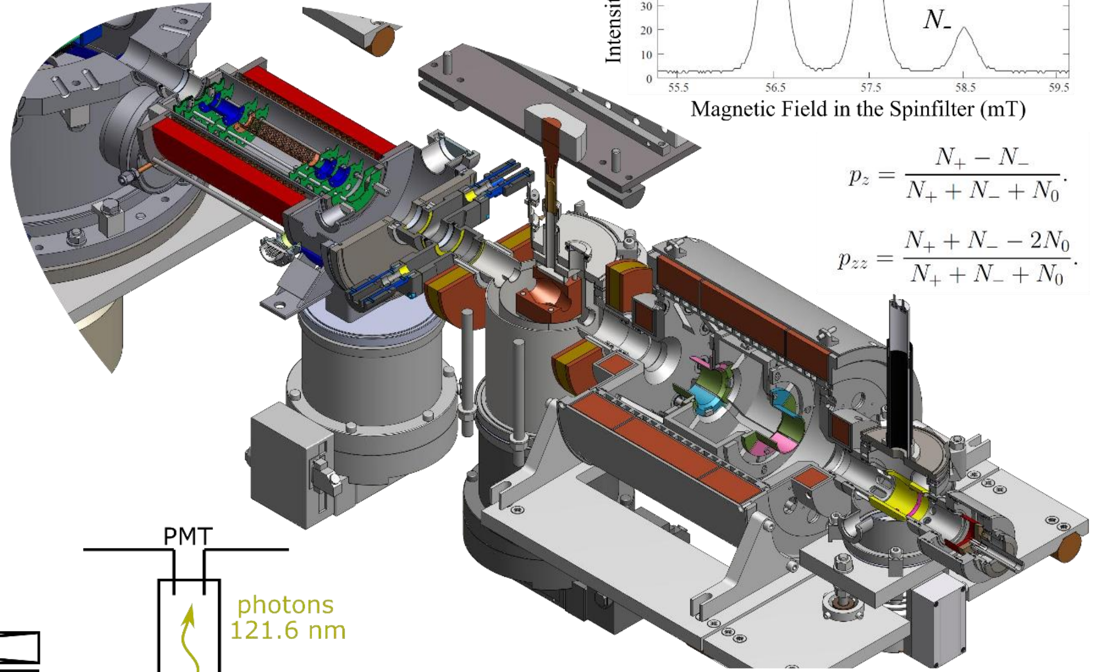

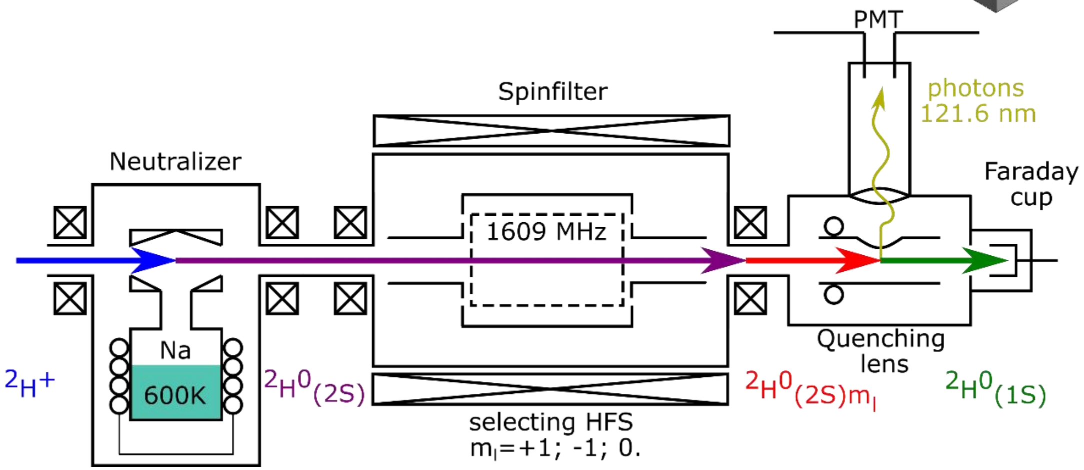

PNPI - NRC KI

$$\frac{L-R}{L+R}=\frac{\frac{3}{2}P_Z\sin\beta\,A_y}{1+\frac{1}{2}P_{ZZ}[\sin^2\beta A_{yy}+\cos^2\beta A_{zz}]}$$

$$\frac{U-D}{U+D}=\frac{P_{ZZ}\sin\beta\,\cos\beta\,A_{xz}}{1+\frac{1}{2}P_{ZZ}[\sin^2\beta A_{xx}+\cos^2\beta A_{zz}]}$$

$$\frac{2(L-R)}{L+R+U+D}=\frac{\frac{3}{2}P_Z\sin\beta\,A_y}{1+\frac{1}{4}P_{ZZ}[3(\cos^2\beta-1)A_{zz}]}$$

$$\frac{2(U-D)}{L+R+U+D}=\frac{P_{ZZ}\sin\beta\,\cos\beta\,A_{xz}}{1+\frac{1}{4}P_{ZZ}[3(\cos^2\beta-1)A_{zz}]}$$

$$\frac{(L+R)-(U+D)}{L+R+U+D}=\frac{-\frac{1}{4}P_{ZZ}\sin^2\beta\,(A_{xx}-A_{yy})}{1+\frac{1}{4}P_{ZZ}[3(\cos^2\beta-1)A_{zz}]},$$

G.G Ohlsen, P.W. Keaton, Jr., Nucl. Instr. and Meth. **109**, 41 (1973).

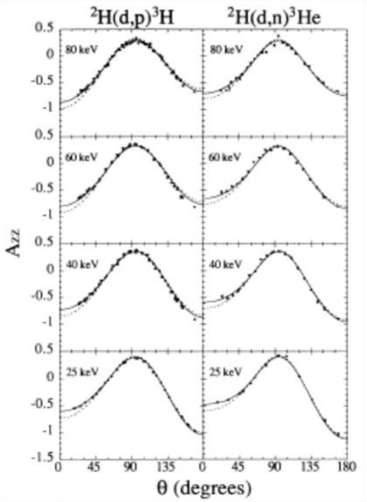

K. Fletcher, *et al.*, Phys. Rev. C **49**, 2305 (1994).

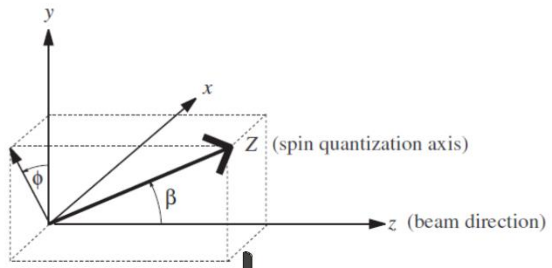

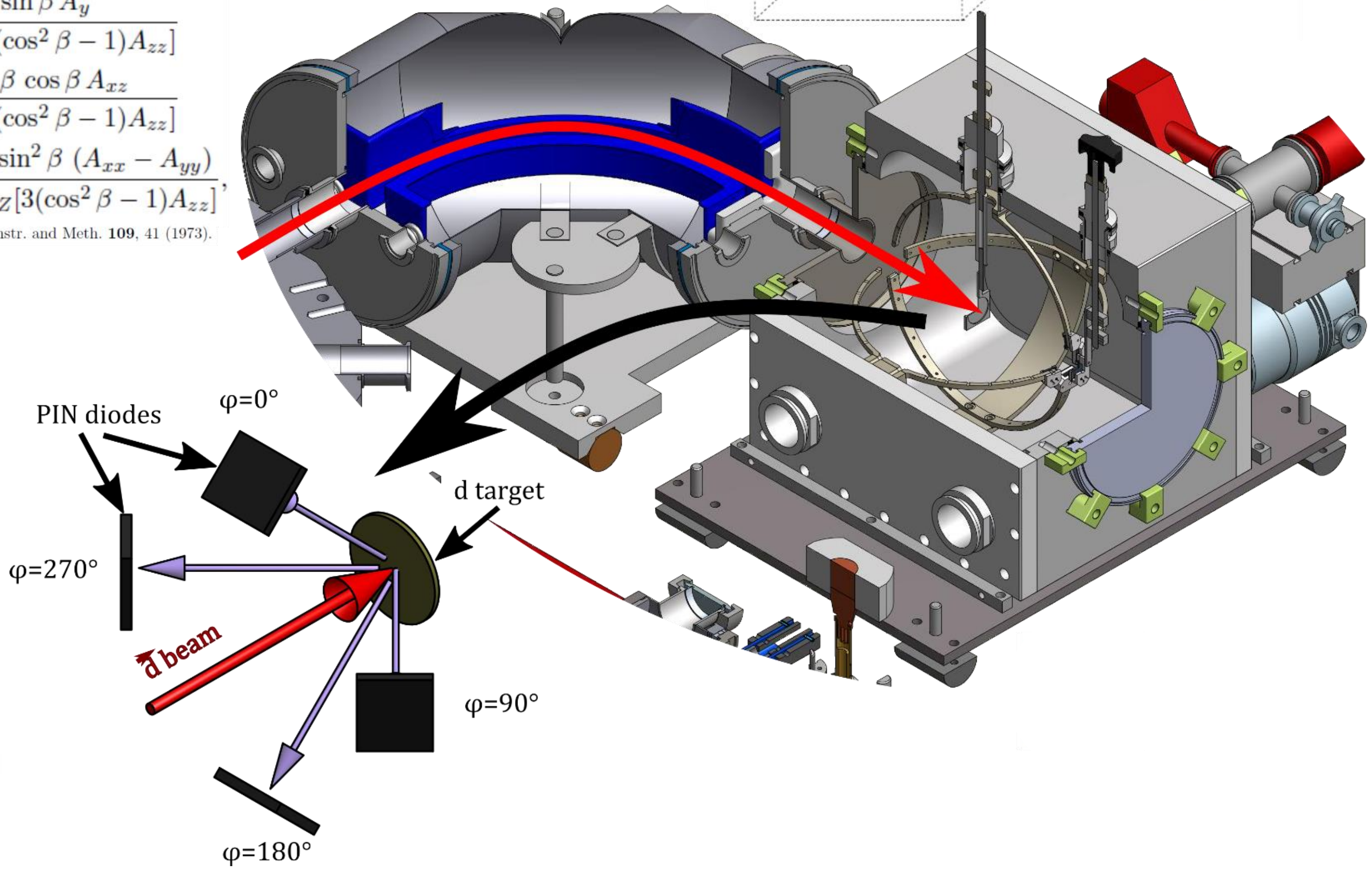

4π - детектор

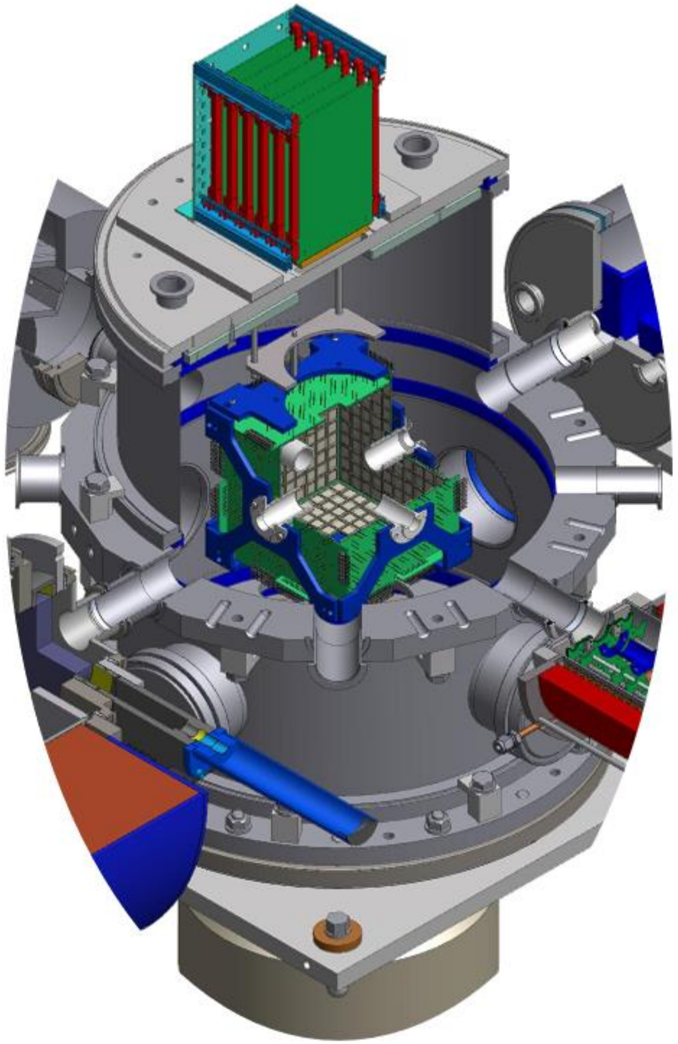

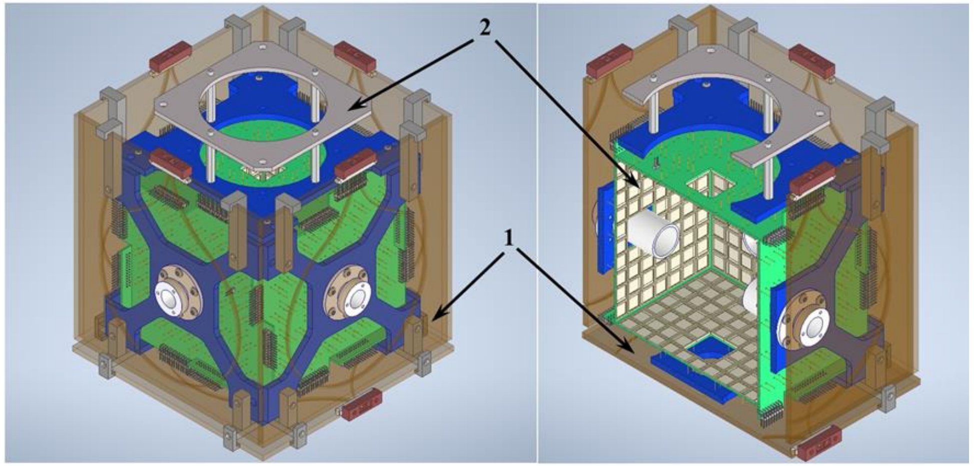

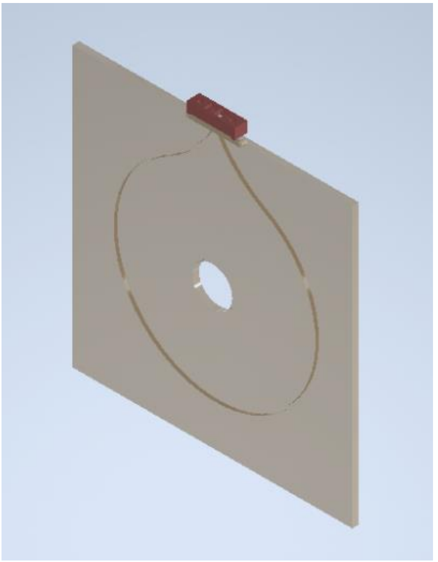

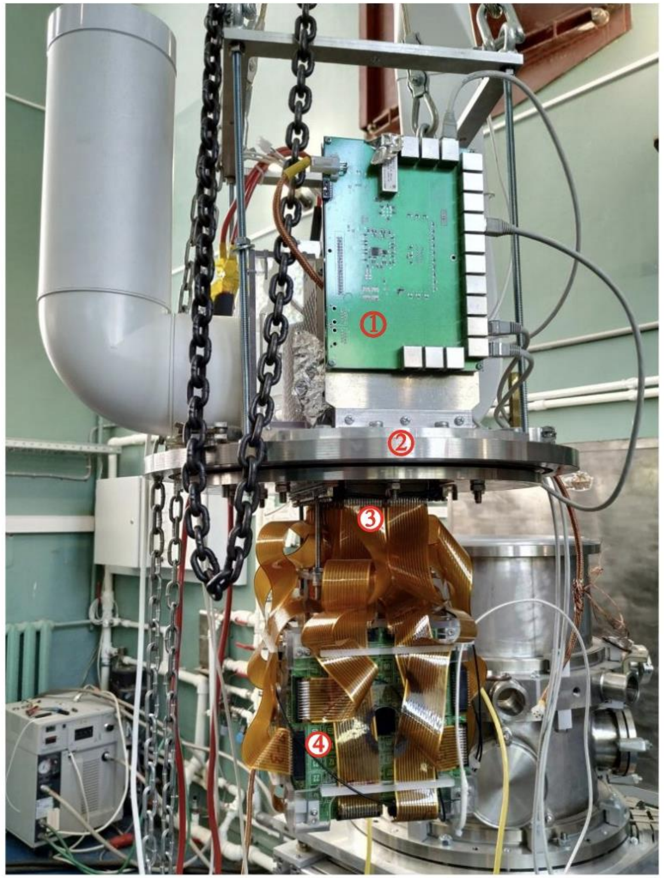

① concentrator
② top flange
③ signal cables
④ detector cube

Сечение реакции

$$
\begin{aligned}
\sigma(\Theta,\Phi) = \sigma_0(\Theta)\{1 \;&+\; \frac{3}{2}\left[A_y^{(b)}(\Theta)p_y + A_y^{(t)}q_y\right] + \frac{1}{2}\left[A_{zz}^{(b)}(\Theta)p_{zz} + A_{zz}^{(t)}(\Theta)q_{zz}\right] \\
&+\; \frac{1}{6}\left[A_{xx-yy}^{(b)}(\Theta)p_{xx-yy} + A_{xx-yy}^{(t)}(\Theta)q_{xx-yy}\right] \\
&+\; \frac{2}{3}\left[A_{xz}^{(b)}(\Theta)p_{xz} + A_{xz}^{(t)}(\Theta)q_{xz}\right] \\
&+\; \frac{9}{4}\left[C_{y,y}(\Theta)p_y q_y + C_{x,x}(\Theta)p_x q_x + C_{x,z}(\Theta)p_x q_z \right.\\
&\quad \left. + C_{z,x}(\Theta)p_z q_x + C_{z,z}(\Theta)p_z q_z\right] \\
&+\; \frac{3}{4}\left[C_{y,zz}(\Theta)p_y q_{zz} + C_{zz,y}(\Theta)p_{zz}q_y\right] \\
&+\; C_{y,xz}(\Theta)p_y q_{xz} + C_{xz,y}(\Theta)p_{xz}q_y + C_{x,yz}(\Theta)p_x q_{yz} \\
&+\; C_{yz,x}(\Theta)p_{yz}q_x + C_{z,yz}(\Theta)p_z q_{yz} + C_{yz,z}(\Theta)p_{yz}q_z \\
&+\; \frac{1}{4}\left[C_{y,xx-yy}(\Theta)p_y q_{xx-yy} + C_{xx-yy,y}(\Theta)p_{xx-yy}q_y \right.\\
&\quad \left. + C_{zz,zz}(\Theta)p_{zz}q_{zz}\right] \\
&+\; \frac{1}{3}\left[C_{zz,xz}(\Theta)p_{zz}q_{xz} + C_{xz,zz}(\Theta)p_{xz}q_{zz}\right] \\
&+\; \frac{1}{12}\left[C_{zz,xx-yy}(\Theta)p_{zz}q_{xx-yy} + C_{xx-yy,zz}(\Theta)p_{xx-yy}q_{zz}\right] \\
&+\; \frac{4}{9}\left[C_{xz,xz}(\Theta)p_{xz}q_{xz} + C_{yz,yz}(\Theta)p_{yz}q_{yz}\right] \\
&+\; \frac{8}{9}\left[C_{xy,yz}(\Theta)p_{xy}q_{yz} + C_{yz,xy}(\Theta)p_{yz}q_{xy}\right] \\
&+\; \frac{16}{9}C_{xy,xy}(\Theta)p_{xy}q_{xy} \\
&+\; \frac{1}{9}\left[C_{xz,xx-yy}(\Theta)p_{xz}q_{xx-yy} + C_{xx-yy,xz}(\Theta)p_{xx-yy}q_{xz}\right] \\
&+\; \frac{1}{36}C_{xx-yy,xx-yy}(\Theta)p_{xx-yy}q_{xx-yy} \\
&+\; \frac{1}{2}\left[C_{x,xy}(\Theta)p_x q_{xy} + C_{xy,x}(\Theta)p_{xy}q_x + C_{z,xy}(\Theta)p_z q_{xy} \right.\\
&\quad \left. + C_{xy,z}(\Theta)p_{xy}q_z\right]\}
\end{aligned}
$$

$p_z(q_z)$, $p_{zz}(q_{zz}) \neq 0$

$$
\begin{aligned}
\sigma(\Theta,\Phi) = \sigma_0(\Theta)\{1 \;&+\; \frac{3}{2}\left[A_{zz}^{(b)}(\Theta)p_{zz} + A_{zz}^{(t)}(\Theta)q_{zz}\right] \\
&+\; \frac{9}{4}C_{z,z}(\Theta)p_z q_z + \frac{1}{4}C_{zz,zz}(\Theta)p_{zz}q_{zz}\}
\end{aligned}
$$

($p_{i,j} \neq 0$, $q_{i,j} = 0$):

$$
\begin{aligned}
\sigma(\Theta,\Phi) = \sigma_0(\Theta) \cdot \{1 &+ 3/2\, A_y(\Theta)\, p_y + 1/2\, A_{xz}(\Theta)\, p_{xz} \\
&+ 1/6\, A_{xx\text{-}yy}(\Theta)\, p_{xx\text{-}zz} \\
&+ 2/3\, A_{zz}(\Theta)\, p_{zz}\}
\end{aligned}
$$

Мотивация

Астрофизика

- Big bang
- Hydrogen burning
- Helium burning
- Advanced burning
- (carbon/neon/oxygen/silicon)
- s-process (neutron sources)
- p-process

Теория ядерного взаимодействия

- Широкий спектр моделей
- Сложности при описании прямых/непрямых измерений

Термоядерная энергетика

- Использованиее поляризованного топлива
- Увеличение сечения
- Управление угловым распределением вылета продуктов реакции
- Реакторы с малым выходом нейтронов

Прикладные аспекты

- Наработка трития и гелия-3
- 3He-ориентированная технология газоразрядных детекторов
- Источник нейтронов для наработки медицинских изотопов 100Mo(n,2n)99Mo

Астрофизика

Big Bang нуклеосинтез ⟶ Первичное распределение изотопов D/H

Вклад ошибки в первичное распределение

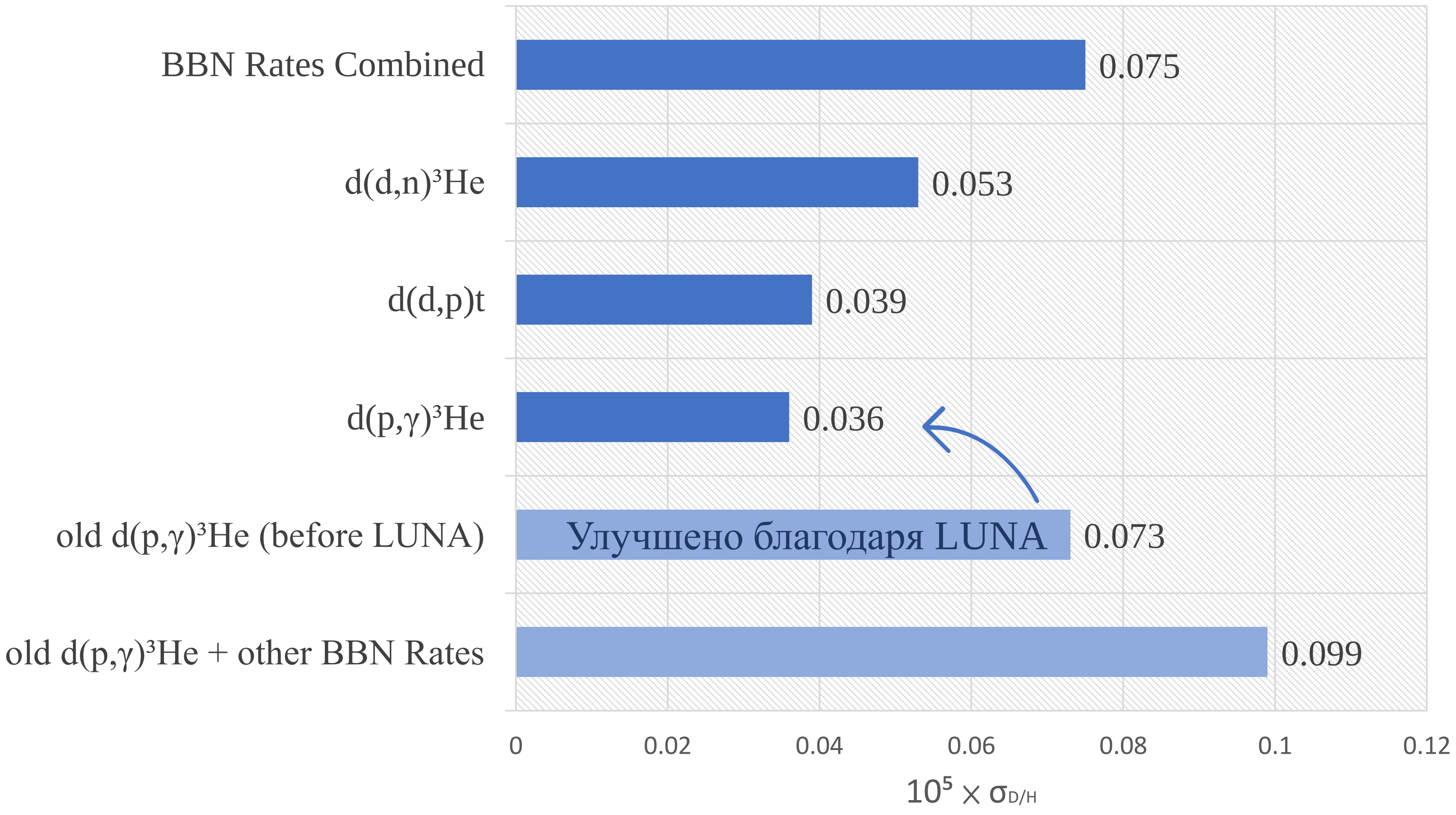

Global BBN Analysis: Tsung-Han Yeh, Keith Olive, Brian Fields (2021)

Необходимы более точные данные по dd-синтезу!

Астрофизика

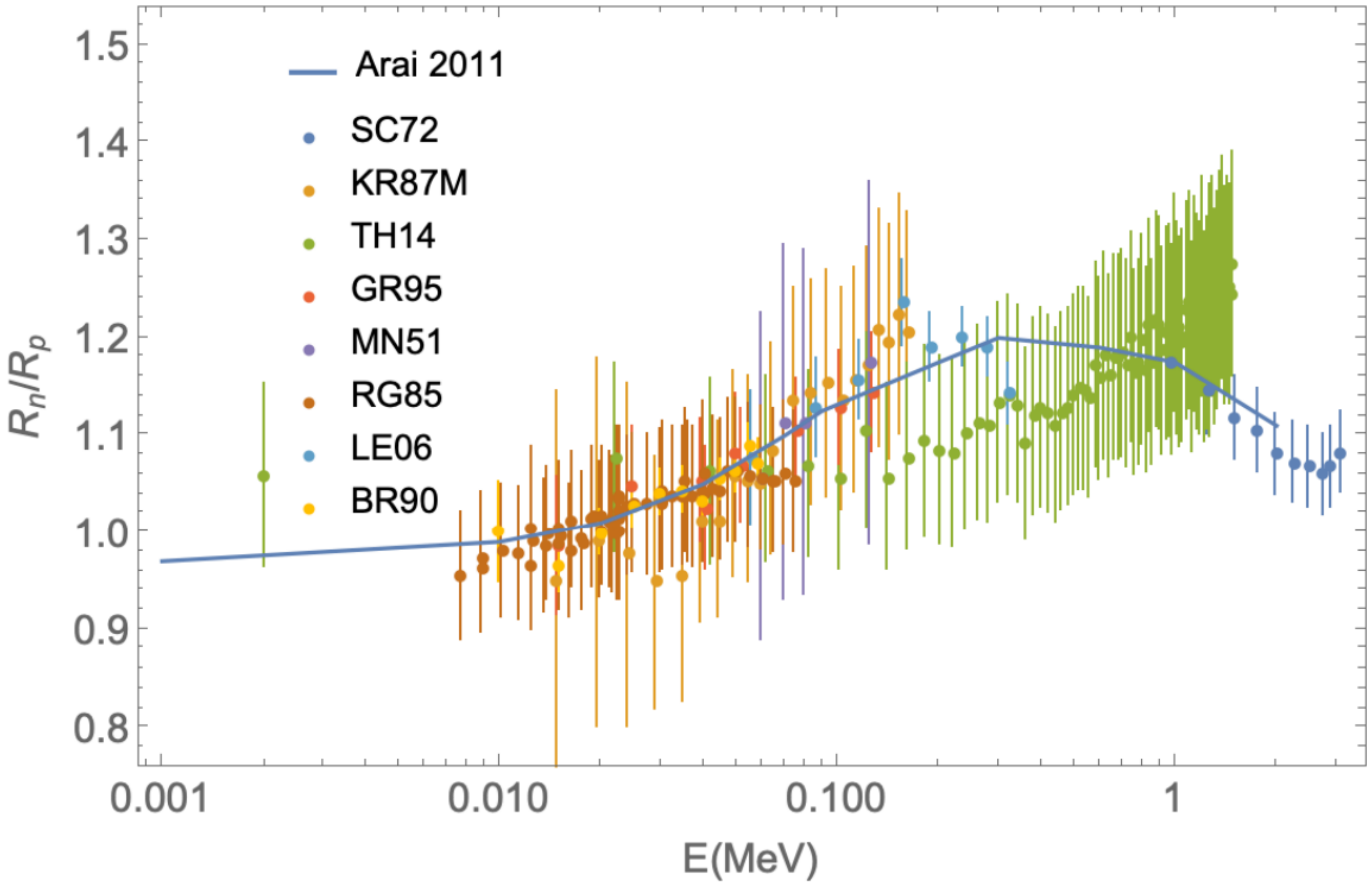

Ofelia Pisanti, Gianpiero Mangano, Gennaro Miele, and Pierpaolo Mazzella Primordial Deuterium after LUNA: concordances and error budget (2020)

Отношения сечений процессов $d(d, n)^3He$ к $d(d, p)^3H$ из экспериментов (точки) и теории (сплошная линия).

Необходимы новые измерения сечения реакции неполяризованного dd-синтеза по обоим каналам!

Теоретическое предсказание:
K. Arai, S. Aoyama, Y. Suzuki, P. Descouvemont, and D. Baye Phys. Rev. Lett. 107, 132502 (2011)

Термоядерный синтез и прикладные аспекты

- Увеличение сечения реакции
- Контроль над направлением разлета продуктов реакции
- Подавление нейтронного канала

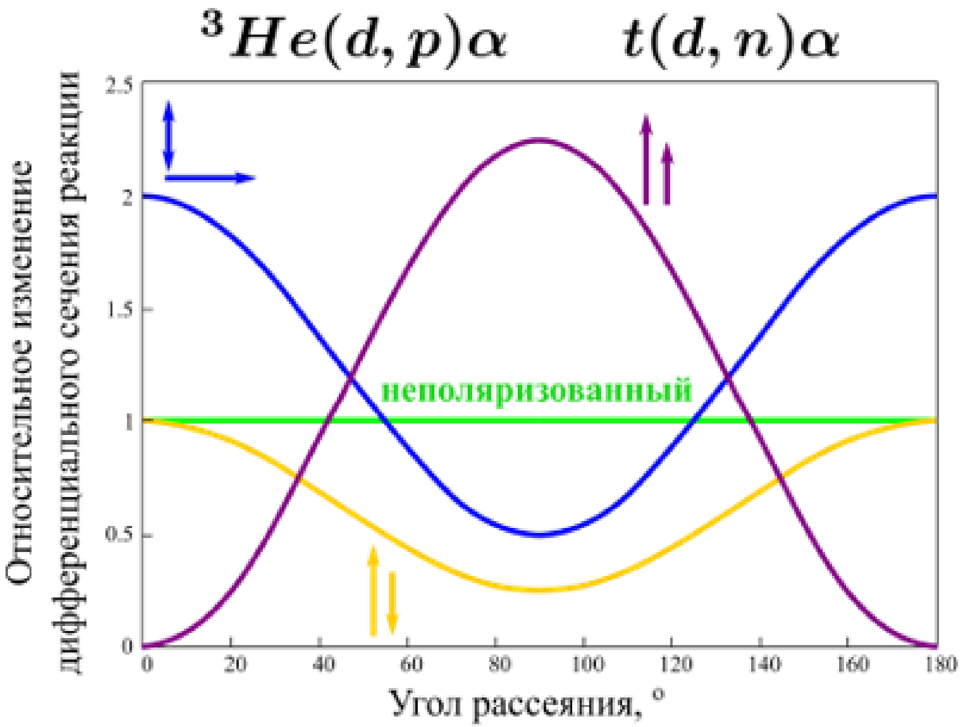

Exp.: Ch. Leemann et al., Helv. Phys. Acta **44**, 141 (1971)
Theor.: G. Hupin et al. Nature Com. **10**, 321 (2019)

Распределения источников нейтронов в координатах (R, Z) для (а) неполяризованного случая и (б) случая полной параллельной поляризации.

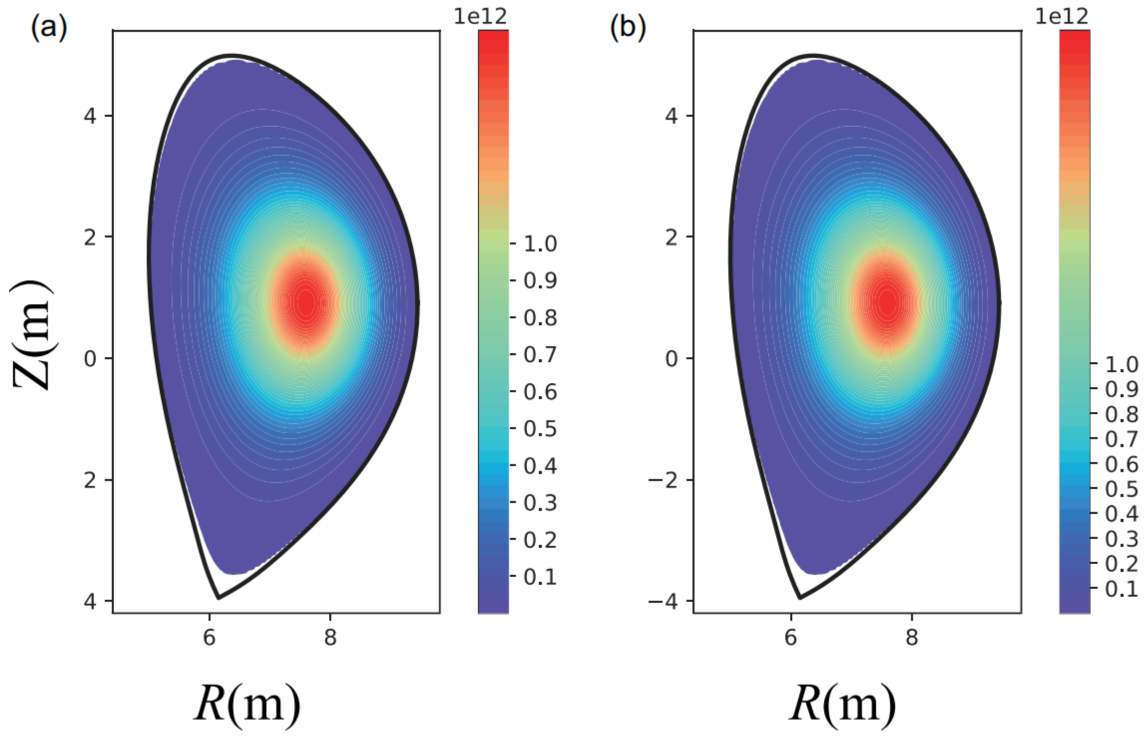

W.Yang, G.Li, X.Gong, X.Gao, X.Li, H.Li… Effect of the Fusion Fuels' Polarization on Neutron Wall Loading Distribution in CFETR (2021) https://doi.org/10.1080/15361055.2021.1969064 (China Fusion Engineering Test Reactor (CFETR))